Reviews in Mineralogy & Geochemistry
Vol. 88 pp. 119-166, 2022

Morphology of Monocrystalline Diamond and its Inclusions

Jeff W. Harris
School of Geographical and Earth Sciences
Gregory Building, University of Glasgow
Glasgow G12 8QQ, U.K.
jeff.harris@glasgow.ac.uk

Karen V. Smit*
Gemological Institute of America
New York City, NY 10128, U.S.A.

Department of Earth and Atmospheric Sciences
University of Alberta
Edmonton T6G 2E3 Alberta, Canada
*Now at the University of the Witwatersrand: *karen.smit@wits.ac.za*

Yana Fedortchouk
Department of Earth and Environmental Sciences,
Dalhousie University, Halifax, Canada
yana@dal.ca

Moreton Moore
Royal Holloway University of London,
Egham, Surrey TW20 0EX, U.K.
m.moore@rhul.ac.uk

INTRODUCTION

Since first being discovered in India over 2000 years ago, the most striking and universally recognized shape of an uncut diamond is the octahedron. This shape was revered from early times, in part because of the hardness of the crystal, but principally because of the ability of that crystal to display a spectrum of color in its uncut state. To ancient people, this property gave the crystal mystical powers and a diamond octahedron soon became a talisman believed to protect the wearer from pestilence or ensure survival in battle. The octahedron reached Europe at the beginning of the Roman Empire (27 BC–AD 476) usually set in gold rings and always in an uncut form. For centuries thereafter diamond was owned exclusively by the nobility and broader ownership developed only after new discoveries in Brazil and South Africa in the 18th and 19th Centuries respectively. Since that time, the octahedron along with other important shapes such as the macle (a twin form), the dodecahedron (a secondary form), and even irregular diamonds, have helped create a world-wide diamond jewelry industry with retail sales worth USD 78.13 billion in 2018 (Tacy 2018).

1529-6466/22/0088-0002$05.00 (print)
1943-2666/22/0088-0002$05.00 (online)
http://dx.doi.org/10.2138/rmg.2022.88.02

For some diamonds, it was not always an easy journey. Once released from their primary rock, diamonds are affected by processes such as dissolution that can change their morphology (e.g., to rounded dodecahedral shapes) and/or impose new surface features. Additionally, about one percent of them had the responsibility of carrying synchronously formed mineral inclusions, subsequently so beloved by diamond researchers. Diamond is, however, an extremely resilient mineral and can survive considerable physical and chemical challenges.

Rough diamonds have a variety of morphologies, surface features, and mineral or fluid inclusions that mean no two rough diamonds are exactly alike. All these features can tell an interesting story of diamond's geological history deep within Earth—both in the mantle rocks where diamonds grew and during their subsequent volcanic transport.

Based on diamond morphology, distinctions can often be made between suites of rough diamonds from different kimberlites (e.g., Harris et al. 1975, 1979). This likely reflects specific mantle regions being sampled during kimberlite eruption, combined with the volatile composition of the kimberlite resulting in specific secondary morphologies. Also, surface features of diamonds are heavily influenced by the composition and temperature of the dissolving fluid/melt, and are another tool that mantle geochemists can use to study carbon-bearing fluids/melts in the deep Earth. Investigating the differences in diamond morphologies and surface features between different kimberlites, therefore, can potentially help geologists understand the compositional variety of kimberlite magmas, getting a step closer to the primary melt composition, which has been a longstanding enigma in mantle geochemistry.

This chapter is divided into four sections and leads the reader through the external and internal morphologies, the surface features and finally the characteristics of the mineral inclusion content of this amazing mineral.

PRIMARY GROWTH MORPHOLOGY

In this section we discuss the morphologies of the principal growth forms of diamond, which can be monocrystalline, twinned, aggregated, irregular, fibrous or coated. These morphologies are illustrated in classic texts, such as Fersmann and Goldschmidt (1911), Sutton (1928), Williams (1932), and Orlov (1977). For information on the morphological characteristics of specific diamond types such as framesite, carbonado and ballas, all usually grouped under the title 'bort', the reader is referred to Jacob and Mikhail (2022, this volume).

Octahedral diamond

The ideal diamond octahedron has eight triangular faces of roughly equal size. Perfect octahedra are relatively rare, and more often diamond octahedra are slightly distorted, elongated or flattened.

Considering its internal crystallographic structure, the octahedron is the expected growth form for diamond. When a crystal grows, atoms adhere to its surface in a regular fashion; and several different kinds of face may be formed. The faces that eventually dominate are those which grow at the slowest rate. This is because fast-growing faces will grow out of the crystal. The slowest-growing faces are usually those that require the greatest number of atoms per unit area (Wulff 1901). For the case of the diamond structure, these are the octahedral {111} planes. Based on this simple model, one might therefore expect all diamond crystals to be octahedra, but this is not so. There are other considerations to take into account: the growing conditions, the local availability of carbon, and the effects of incorporated defects, such as dislocations enhancing growth rates. There are indeed countless natural diamonds that are octahedral, but there are many other shapes, to be discussed below. Some typical octahedral diamonds are shown in Figure 1.

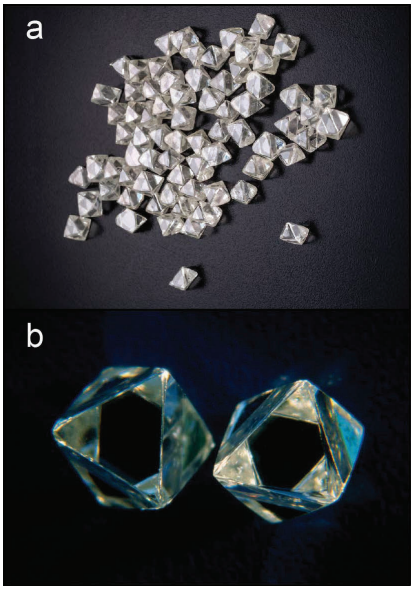

Figure 1. Octahedral diamond crystals. **(a)** Rough octahedral diamonds from Jwaneng, all in the 3 ct range. **(b)** Two unusually sharp-edged and equant 1 ct octahedral diamonds from Angola. A 1 carat octahedron has an edge length of approximately 5 mm. [Image in (a) reproduced from Weldon and Shor (2014), Gems and Gemology. Used with permission. Image in (b) courtesy of Thomas Hunn Co.]

Diamonds of cubic habit

The second monocrystalline primary form of diamond is the cube whose occurrence is rarer than the octahedron but is not uncommon. Cubic diamonds are found in production from Brazil, Siberia, Sierra Leone, the Democratic Republic of the Congo, South Africa and Botswana.

Gem cubes in the size range 2–6 mm from Botswana are not usually well-shaped, nor are their surfaces flat. In many instances these surfaces are associated with cube edges which are distinctly rounded, but with well-developed striations set at right-angles to these edges: see Fersmann and Goldschmidt (1911) for examples. In the 2–4 mm size range for diamonds from Siberia (Fig. 2; Zedgenizov et al. 2016) shapes are similar but striated edges appear to be absent.

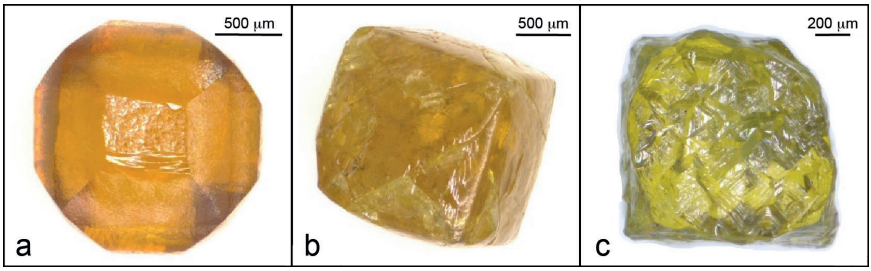

Figure 2. Irregular orange and yellow cuboid alluvial diamonds from NE Siberia. [Images by Dmitry Zedgenizov (Sobolev Institute of Geology and Mineralogy).]

As curved cube faces can be inclined up to 30° from true cubic directions (Lang 1974a; Suzuki and Lang 1976) and because of all their other characteristics, diamonds with this habit are better termed ‘cuboid’. Within the smaller diamond sizes (1–2 mm) flat faced and more regular shaped cubes exist and these can have translucent or opaque diamond coats. They are found particularly in the Mbuji Mayi production from the Democratic Republic of Congo (DRC) (Fig. 3), but also in diamonds from Sierra Leone (Grantham and Allen 1960) and Wawa, Canada (Stachel et al. 2006). With the larger gem diamonds their characteristics contrast with

the planar cube faces often found on synthetic diamonds, especially in combination with octahedral faces in the latter. The relative development of the two forms, {100} and {111} can be varied by changing the temperature (Bovenkerk 1961; Yamaoka et al. 1977), and cooler conditions favor growth of cubic faces. The temperature can be adjusted to create synthetic diamonds in the shape of a cubo-octahedron (Moore 1985), which is a 'blocky' morphology chosen for industrial sawing applications. A review contrasting the morphologies of natural and synthetic diamonds has been written by Sunagawa (1995).

A second cube form of diamond is the result of fibrous octahedral growth. The resultant opaque cube shape can be regular with flat faces, edges being slightly rounded. For details on how both types of cuboid diamond grow, see Moore and Lang (1972) and the *Internal Morphology* section below.

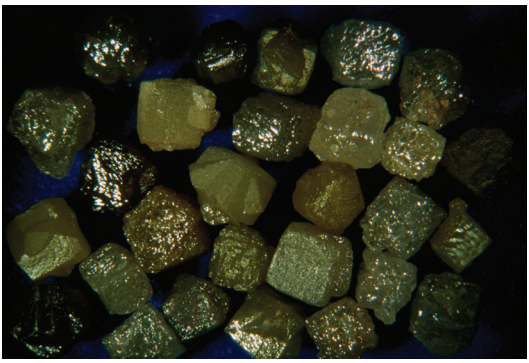

Figure 3. 70 carats of rough cubic diamonds from the Democratic Republic of Congo, with an interpenetrant twin in the center. [Image courtesy of Thomas Hunn Co.]

Mixed-habit diamonds with cubo-octahedral morphology

There is clear evidence that some more moderately sized diamonds have shapes that are the result of a mutual growth between octahedron and cube. Invariably in these cases, octahedral growth is faceted whilst that of the cube is curved and non-faceted. If one direction is progressively dominant over the other, then the resulting shape may be an octahedron or a cube, but the internal structure, as seen by cathodoluminescence, identifies the two contributions (see *Internal Morphology*). If one of the directions is distinctly faster, gem cubes, for example, may have prominent octahedral corners or have pronounced edges giving the diamond a distinct skeletal appearance, sometimes referred to as re-entrant cubes (Tappert and Tappert 2011).

In shape classification studies on Botswanan diamonds in the 2–6 mm size range, a small but noticeable proportion of mixed-habit diamonds were recorded in the non-industrial diamond fraction (Harris et al. 1986). At Jwaneng they took the form of cubo-octahedra and cubo-dodecahedra, whilst at Orapa they were cubo-dodecahedra only, this shape in both localities being a consequence of dissolution. In similar work on South African diamonds (Harris et al. 1979), cubo-octahedra were occasionally recorded from the 1 mm fraction at the Cullinan (formerly Premier) mine.

Coated stones

When fibrous growth (characterized by fibers branching in <111> directions) occurs from the surface of an octahedral diamond, already formed by faceted {111} growth, then a 'coated stone' is the result (Kamiya and Lang 1965). Why a growing diamond should change from faceted growth to fibrous growth is still a topic for discussion, but clearly it indicates a marked change in growth conditions. Impurities incorporated during growth could be partially

responsible for the change in growth directions. These impurities attach themselves to the growing surface and prevent the lateral spread of diamond growth parallel to {111} planes and the formation of smooth faces. In some specimens, X-ray topographs revealed not only the sharp interface between the good-quality octahedral 'core' and the 'coat' but also several successive epochs of fibrous growth (Fig. 4). Since the fibers grow perpendicularly from these octahedral faces, the resultant faces on the coated stone are also triangles: maintaining the same size, shape and orientation as the triangular faces on the 'core' diamond. The size of the 'core' may therefore be simply determined by measuring the slant edge lengths of the coated stone, which are equal to the edge-lengths of the octahedron (Machado et al. 1985). An interested jeweler can cleave off the imperfect coat material on {111} planes to reveal the gem inside!

In addition to octahedral faces, a coated stone may also exhibit cube faces and dodecahedral faces, ideally forming a rhombicuboctahedron (Machado et al. 1985). The six cube faces grow from the six corners of the octahedron by fibrous growth in four octahedral directions. The twelve dodecahedral faces have grown from the twelve edges of the octahedron, each in just two directions. For example, the (110) face is made from fibers running in [111] and [11$\bar{1}$] directions. Close examination of these dodecahedral faces by scanning electron microscopy showed that they are not flat but finely corrugated, with the sloping sides parallel to {111}. Some sides have been seen to have trigons upon them, confirming their assignment to {111}. The dodecahedral form {110} is therefore not a true growth form for natural diamond (although it is sometimes reported for synthetic diamond). The faces, being made up of fine-scale {111} surfaces, may be described as 'pseudo-dodecahedral'.

Coated diamonds are principally found in the production from the DRC (Kamiya and Lang 1965; Boyd et al. 1987; Akagi and Masuda 1988; Navon et al. 1988), although noticeable amounts are recovered from Sierra Leone and Canada (Grantham and Allen 1960; Gurney et al. 2004; Yelisseyev et al. 2004; Petts et al. 2016).

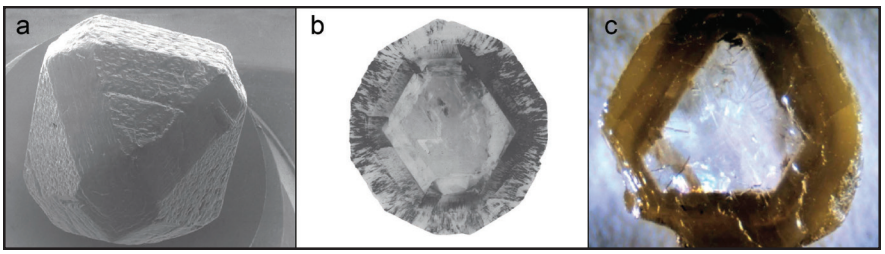

Figure 4. Faceted growth followed by fibrous growth. (**a**) Secondary electron image of a cubo-octa-dodec diamond with 8 mm diameter (**b**) Section X-ray topograph of the same diamond showing multiple layers of fibrous growth. (**c**) A coated stone from Sierra Leone (4 mm across) showing a clear center and distinct growth layering within the coat. [Images in (a,b) reprinted from Machado et al. (1985). Image in (c) by Jeff Harris.]

Tetrahedral diamond

Ever since Bragg and Bragg (1913, 1914) determined the crystal structure of diamond, most scientists have accepted that its point group symmetry is $\frac{4}{m}\bar{3}\frac{2}{m}$ (that is, cubic holosymmetry). Very occasionally natural diamonds have been found that have the appearance of being tetrahedra and these are illustrated in the classic works of Fersmann and Goldschmidt (1911), Sutton (1928) and Williams (1932). If primary, the existence of tetrahedral diamond changes the point group symmetry to the hemihedral class $\bar{4}3m$; and therefore to a class that does not have a center of symmetry. For this to be true, the tetrahedral habit would have to be a growth form arising from unimpeded growth from a center, resulting from internal inter-atomic forces; rather than acquired by external events such as fracture, cleavage along {111}, plastic deformation or dissolution.

Seager (1979) made a careful study of one such diamond and noted that whereas three of the four 'tetrahedral faces' were similar in appearance, the fourth was quite different. Using high-resolution X-ray topography to probe the interiors of 11 diamonds, Yacoot and Moore (1993) concluded that the tetrahedral diamonds studied were {111} cleavage fragments from larger stones, sometimes together with twinning from the origin on one, or two non-parallel, {111} planes. No diamonds have been found that actually grew as flat-faced tetrahedra, and thus the diamond structure remains firmly in the category of the cubic holosymmetric point group $\frac{4}{m}\,\bar{3}\,\frac{2}{m}$.

Diamond twins and aggregates

Twinned crystals. Instead of single-crystals, natural diamond can also grow as pairs of twins that are aligned along crystallographic planes. There are two main varieties: contact ('spinel-type') twins for faceted octahedral growth and interpenetrant ('fluorite-type') cubes for fibrous growth. Twinning of diamonds formed by cuboid growth has not been reported.

Because diamond possesses full cubic symmetry, twinning in diamond by a 180° rotation about a [111] direction is the same as twinning by a reflection in a (111) plane. *Contact twins* therefore develop by faceted growth on {111} planes and are known as 'macles' in the diamond trade (Fig. 5). They are often of a thin triangular shape with small re-entrants at the corners; and the twin plane is not always planar but often shows some inter-growth (Yacoot et al. 1998). These authors also found that the origin of contact-twinning is nearly always at the center of the diamond and this is often marked by a visible inclusion (see *Internal Morphology* section below). *Interpenetrant cubes* are rare, and they are usually colored yellow or brown. In the few specimens examined, twinning appears to have started from the center (Machado et al. 1998).

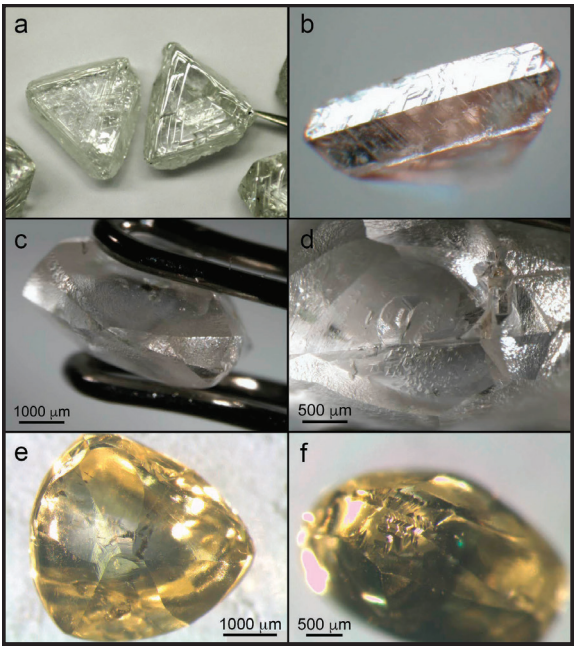

Figure 5. Features of typical macles. (**a**) A set of slightly dissolved (resorbed) macles with the arm of tweezers for scale. (**b**) A single macle showing a straight twin plane with characteristic herring-bone, with scale the same as in (a). (**c**) A dodecahedral macle showing the truncation of the dodecahedroid faces by the macle line. (**d**) A stepped macle plane. (**e**) A dissolved macle with an obvious medial line indicating a tetrahexahedroid (THH) crystal. (**f**) A thicker THH macle. [Images (a, b) used with permission of Anetta Banas (University of Alberta). Images (c-f) by Karen Smit.]

Multiple twinning on {111} planes can produce interesting and beautiful morphologies in natural diamond. A 'Star of David' morphology can form by the combined growth of two macles, the flat faces of which are in contact and the triangular outlines being oriented in opposite directions (Fig. 6). The angular relationship between these two macles is a rotation of 180° about the common [111] normal to the parallel twin planes.

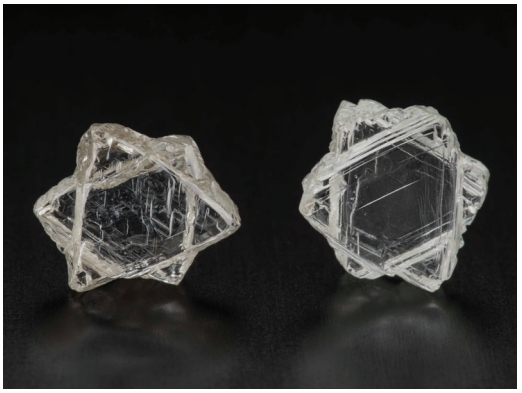

Figure 6. 'Star of David' diamonds—six-pointed star-shaped contact twins. Left diamond is 0.92 ct (6.15 × 6.84 × 2.66 mm); right diamond is 0.98 ct (6.48 × 6.66 × 2.45 mm). [Image by Robert Weldon (GIA). Diamonds courtesy of Trillion Diamond Company, NY.]

When twinning occurs on non-parallel planes, a cyclic twin (or 'star twin') can result. Such twins are not uncommon among synthetic diamonds, but they are rather rare in natural stones. The angle between two {111} planes is approximately 70.5°. This means that five twinned crystals can grow around a common [110] axis, with some room to spare: 5 × 70.5 = 352.5°, leaving a narrow diamond wedge of angular thickness of approximately 7.5° (to complete the full circle of 360°), see Fersman (1955).

Diamond aggregates. Two or more intergrown diamonds can also be aggregate crystals (Fig. 7). They can be distinguished from twinned diamonds if there is a lack of crystallographic alignment between crystals. However, there are some examples where (now) octahedral diamonds started as aggregates showing crystallographic alignment (Fig. 8).

Figure 7. Aggregate of octahedral crystals. [Image by Karen Smit.]

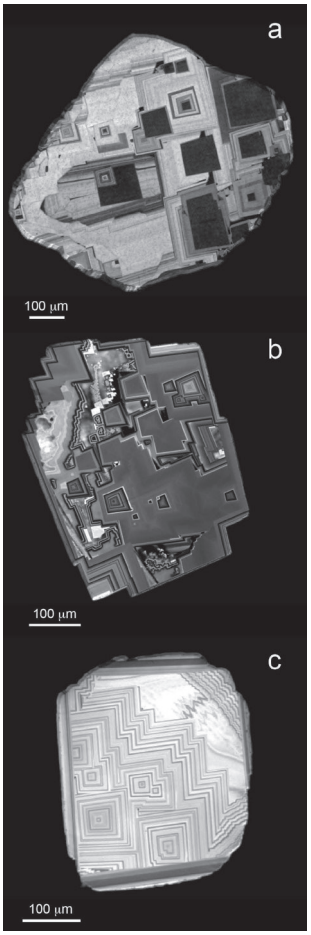

Figure 8. Cathodoluminescence of the internal growth features show that these (now octahedral) Ekati diamonds probably started as aggregates, and show that aggregates may have crystallographic alignment. [Images in (a,b) by Zhihai Zhang (Dalhousie University). Image in (c) from Zhang (2016).]

Irregular diamonds

Some diamonds show little or no discernible morphology. If the shape is fracture controlled then such diamonds can be divided into two groups: those that have broken in the kimberlite or lamproite and whose edges have been rounded by later dissolution (old breaks), or those whose edges are still sharp (new breaks) and which probably resulted from damage during diamond recovery or in an alluvial environment.

At high temperatures above 900°C, diamond deformation is typically ductile, so just how diamonds fracture in the igneous environment is uncertain, but Clement et al. (1986) showed that explosive or implosive brecciation occurred directly around parts of the root zone of the De Beers mine in Kimberley. The authors considered the angular breccia to be a consequence of *in situ* shattering of the country rock by a precursor gas phase. If this kind of event occurred more generally during or just after eruption, when the kimberlite was cooling, then shock waves from such explosions might fracture a proportion of the diamond content, over a range of near surface depths.

If an irregular diamond is without obvious fractures, then the shape is principally controlled by dissolution. Diamonds in this category are not uncommon and many large sub-lithospheric diamonds have irregular shapes, such as the newly-recognized CLIPPIR diamonds (Cullinan-like Large Inclusion-Poor, relatively Pure, Irregularly shaped, Resorbed diamonds; (Smith et al. 2016b, 2017). A specific source for these large diamonds is the Letšeng-la-terae mine in Lesotho (now commonly shortened and called the Letšeng mine, Shor et al. 2015). The irregular nature of sub-lithospheric diamonds could be due to sequences of breakage and dissolution in the deep Earth. Deep Focus Earthquakes (Zhan 2020), show that brittle deformation is indeed possible at such depths. Sub-lithospheric diamonds often have rounded, irregular and complex surfaces (Fig. 9).

Figure 9. Faint pink (3.72 ct) and greyish blue (9.55 ct) irregular diamonds from the Letšeng mine in Lesotho. [Reprinted from Shor et al. (2015) Gems and Gemology. Used with permission.]

SECONDARY MORPHOLOGIES OF DIAMOND

When diamonds are recovered from mantle xenoliths, those that are completely enclosed in the xenolith are invariably sharp-edged. Robinson (1979) considered this to be particularly true for diamonds in eclogitic xenoliths. Although the majority of diamonds recovered directly from xenoliths are octahedra or macles, cube-shaped microdiamonds (0.5 mm) have been recovered from eclogitic xenoliths from Udachnaya (Spetsius 1998). Once released from xenoliths, these diamond shapes can remain pristine and show very little attack (or dissolution) by fluids either during mantle storage or during kimberlite transport. In other instances, diamonds are transformed from their primary shapes into secondary shapes by fluid dissolution. Changes induced by dissolution are progressive: for octahedra, the results of this process are recognized as dodecahedroids or tetrahexahedroids (THH) and for macles, the end-products are pin-cushion macles (Fig. 10).

A century-old controversy as to whether the dodecahedral shape was a growth form or the result of dissolution from larger stones was settled by Moore and Lang (1974). They used X-ray topography (XRT) of the internal growth surfaces within dozens of dodecahedra to show that the dissolution of octahedral diamonds was responsible for turning the twelve edges of the octahedron into the twelve rounded pseudo-faces of the rhombic dodecahedron. The concentric 'growth horizons' within each diamond were one-time external surfaces of the crystal; and their octahedral shape resulted from good faceted growth. They are visible in XRT because strain-producing particles have altered the lattice parameter by a few parts per million. These strain-producing particles may be the result of impurities incorporated during crystal growth.

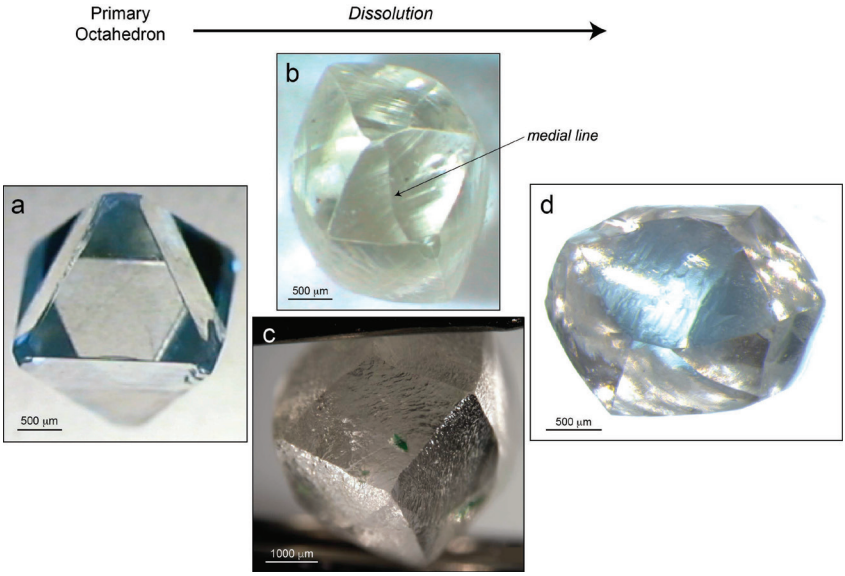

Figure 10. The sequence of dissolution from an octahedron (**a**) to a tetrahexahedroid (THH) (**d**). During dissolution, each octahedral face is reduced to a vertex surrounded by three rhombi to form a dodecahedroid. Across each short diagonal of a rhombus is a sinuous medial line. If this medial line is regarded as a divide between two faces then the resulting polyhedron is best described as a tetrahexahedron {*hk*0} (**b**). If that line is not regarded as a face edge but just a minor feature, and the rhombi are flatter, then the polyhedron is a dodecahedron (**c**). For both crystals, further dissolution creates more rounded THHs (**d**). Neither of these secondary shapes has true crystal faces, but rather curved dissolved surfaces that only approximate similar crystallographic directions to crystal faces, and accordingly the crystal names end with "-oid". [Images in (a,b) by Jeff Harris. Image in (c) by Karen Smit. Image in (d) by Yana Fedortchouk.]

The outermost growth horizons are truncated by the present external surface of each diamond, unequivocally demonstrating that the crystal was once bigger than it is now; and that the rhombic dodecahedral form is a dissolution shape. Furthermore, differential etching of growth horizons with different impurity concentrations has caused many of the diamonds to have terraces surrounding their triad axes (see *Surface Features s*ection).

The manner by which dissolution proceeds can be described on an atomic scale by the motion of kinks along stable monomolecular steps parallel to <110> directions. Each rhombic 'face' is often comprised of two parts, with a common boundary running along the minor diagonal of the rhombus. Unlike the rhombus edge, this minor diagonal (known as the medial line) is usually sinuous and rarely intersects the triple points at either end of the short diagonals of the rhombus. The line may be regarded as the intersection of two solution fronts starting from two four-fold apices of the original octahedron.

If this medial line is not regarded as a face edge but just a minor feature, then the polyhedron is a dodecahedron. If the medial line is regarded as a divide between two faces then the resulting polyhedron is best described as a tetrahexahedron {*hk*0}. For easier visualization, these forms can be considered as a theoretical morphological spectrum with the dodecahedron and cube as end-points, *although it is emphasized that cubes do not form in this way*. The dodecahedron is bounded by 12 rhombic (lozenge-shaped) faces, each of which may be considered as being composed of two triangles divided by the minor diagonal. Considering the two triangles to bend about the minor diagonal and the angle between their normals to increase, the morphology transforms from dodecahedron with zero angle to dodecahedroid, then THH, and finally a cube.

Neither of these secondary shapes has true crystal faces, but rather curved dissolved surfaces that approximate similar crystallographic directions to crystal faces. To account for the curved surfaces for both these shapes, they are termed hereafter as tetrahexahedroids (THHs—with 24 dissolved surfaces) and dodecahedroids (with 12 dissolved surfaces). When remnants of octahedral faces are present on these rounded diamonds, they show trigonal shapes on dodecahedroids and ditrigonal shapes on THHs. Examples of dodecahedroids and THHs are shown in Figures 11 and 12.

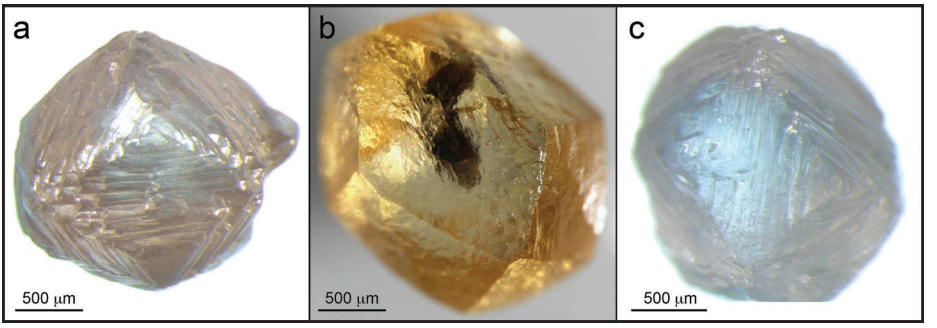

Figure 11. Further examples of dodecahedroid crystals. [Image in (a,c) by Yana Fedortchouk. Image in (b) by Karen Smit.]

An ongoing debate concerns how much importance is placed on the medial line. For example, Orlov (1977) used dodecahedroid in his descriptions of Russian diamonds. In shape classifications of diamonds from the major mines in South Africa and Botswana, Harris et al. (1979, 1986) used dodecahedron, whilst Robinson et al. (1989) favored THH. Recent surface feature work on Canadian diamonds also used THH (Fedortchouk 2019).

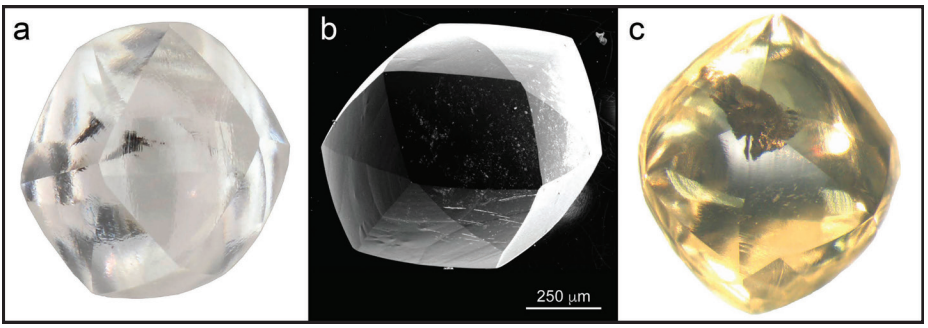

Figure 12. Further examples of tetrahexahedroid (THH) crystals. [Image in (a) by Jian Xin (Jae) Liao (GIA). Image in (b) by Yana Fedortchouk. Image in (c) by Karen Smit.]

Macles undergo the same dissolution as the octahedron, but the process is constrained by the twin plane. Either side of that plane, the original octahedral surfaces eventually divide into three curved faces with medial lines that are all closed off by the twin divide. Nevertheless, the resulting surfaces exhibit all the features found on dodecahedroid surfaces. Figure 5c–f shows some typical macles that have undergone dissolution.

Dodecahedroid and tetrahexahedroid (THH) formation conditions

Early work by Chepurov et al. (1985) on how mafic silicate melts dissolved diamonds at high pressure, was followed by further studies mostly in the noughties (2000–2009). Most of the new work involved varying amounts of H_2O and/or CO_2 in starting materials of natural kimberlite or lamproite (Kozai and Arima 2005), carbonate and silicate melts (Khokhryakov and Pal'yanov 2007, 2010), or H_2O- and CO_2-fluids (Fedortchouk et al. 2007). Pressure conditions for these experiments covered the range for diamond occurrence in the sub-cratonic lithospheric mantle—between 1 and 7.5 GPa and temperatures between 1150 and 1750 °C.

Invariably the diamond products were referred to as dodecahedroids or THHs, but images show that some of the resultant diamond shapes were difficult to clearly define, although authors attempted to do so. Khokhryakov and Pal'yanov (2007) and Fedortchouk et al. (2007), however, show dissolved diamonds where the 'medial line' is straight and connected to the triple points either side of the short diagonal of a rhombus. In both sets of experiments, the THHs formed by dissolution in a carbonate/water mix.

The experiments by Khokhryakov and Pal'yanov (2007, 2010) were conducted mostly at 5.7 GPa and 1400 °C. These temperatures are somewhat higher than the average diamond formation conditions in the cratonic lithosphere (Stachel and Luth 2015) and they argued strongly that all dissolution of diamond took place in the mantle, principally because late-stage changes would not be compatible with the short eruption times from mantle depths. On the other hand, the experiments by Fedortchouk et al. (2007) showed that serious dissolution took place within hours at 1 GPa and 1150–1500 °C, suggesting dissolution of diamond during the late stages of kimberlite eruption was possible. Fedortchouk and Zhang (2011) considered that dodecahedroid formation occurred in the mantle, whereas THHs were late-stage alteration products of dodecahedroids. Dissolution and formation of THHs occurred during kimberlite ascent, and it was severe enough to leave very few dodecahedroids.

Earlier studies of diamond shape from southern African sources mostly reported dodecahedroids. A possible solution to the dilemma of why THHs were not commonly found may relate to differences in the diamond sizes studied: the southern Africa studies (Harris et al. 1979, 1983) were on 2–6 mm diamonds whereas those that reported THHs were on ~1 mm Canadian microdiamonds (Fedortchouk and Zhang 2011). Late-stage dissolution on a small dodecahedroid would have a greater ability to change the shape into a THH than a similar level of dissolution on a larger similar diamond.

Figure 13 is an example of a so-called pseudohemimorphic diamond (named by Robinson 1979) that appears to be in two parts, a dodecahedroid top and an octahedral bottom. However, the diamond is a single crystal that shares the same axes and has identical color between the two halves. Pseudohemimorphic diamonds are not common, although they were noticeable in the production from the Venetia mine in South Africa (Jeff Harris, personal observation). These diamonds result from partial dissolution of an original octahedron, where portions of the diamond are protected from dissolution by kimberlite fluids, by being partly embedded in another mineral or xenolith.

Figure 13. A 2–3 mm partially dissolved (resorbed) pseudohemimorphic South African diamond displaying a dodecahedroid top and pristine octahedral lower portion. [Image by Jeff Harris.]

INTERNAL FEATURES OF DIAMOND

In general, diamond has a complex internal growth history. In the early days, the internal growth features were examined after etching with potassium nitrate at temperatures around 575 °C or using X-ray topographic techniques. For details of the diverse X-ray techniques that can be used to examine the interior of diamonds see Moore (2009) and references therein. The most common modern technique to investigate diamond growth history is through cathodoluminescence (CL) imaging, that is created by luminescence instrumentation attached to optical microscopes, and instruments such as scanning electron microscopes (SEMs). Instruments such as the DiamondView™ that use UV rather than electron excitation can also be used to create luminescence images (Welbourn et al. 1996).

Initially the study of diamond plates by some of the above methods was the realm of physicists who wished to determine and locate defects, such as dislocations or stacking faults in diamond crystals, particularly synthetic ones. The patterns exposed by these techniques however, were also used to elucidate the way natural diamond grows, much of the initial work being completed in the second half of the 20th century. Notable amongst this work was that of Seal (1965) who studied 86 diamonds from mines in seven countries and discovered virtually all the main types of growth patterns.

Influence of nitrogen content on internal features

An important factor that influences many of the internal features we see in diamond is the presence or absence of nitrogen, where nitrogen-containing (>5 at. ppm) diamonds are termed Type I, and nitrogen-free (<5 at. ppm) diamonds are Type II. The absence of nitrogen in Type IIa (nitrogen- and boron-free) and IIb (boron-containing) diamonds lessens the yield stress by a factor of two, relative to Type I diamonds (Evans and Wild 1965). Consequently, Type II diamonds plastically deform more easily than Type I diamonds.

The influence of nitrogen on the internal strength of diamond was demonstrated for half-colorless half-brown diamonds from the Argyle mine in Australia (Nailer et al. 2007). Colorless zones had 1.6× more nitrogen than brown zones, yet clearly the two halves of each diamond would have experienced exactly the same pressure, temperature, and stress conditions. The presence of nitrogen, therefore, stiffened the diamond against natural plastic deformation, and the nitrogen-rich sectors remained colorless whereas the nitrogen-poor sectors became brown due to deformation (Fig. 14).

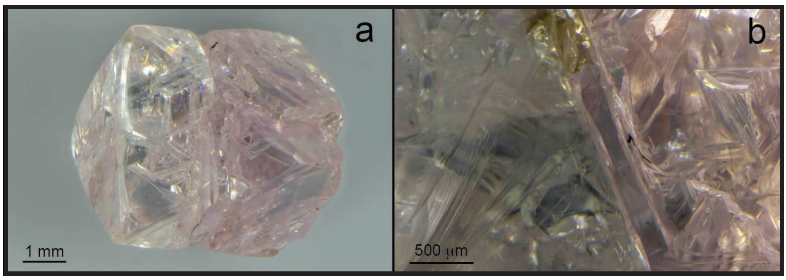

Figure 14. Half-colorless, half-pink aggregate diamond from Argyle (Australia). Higher nitrogen content in the colorless diamond is thought to stiffen the diamond against natural plastic deformation, also observed in other Argyle diamonds by Nailer et al. (2007). [Images by Sally Eaton-Magaña (GIA).]

The relative resilience of Type I diamond to stress fields does nevertheless cause some plastic deformation, frequently observed as deformation slip planes or deformation twins, though the original growth patterns are preserved (see *Surface Textures* section below). On the contrary, Type IIa and IIb diamonds show almost ubiquitous deformation. Deformation starts through the introduction of lattice dislocations, and with subsequent prolonged mantle annealing, these dislocations migrate through the crystal to form dislocation loops which polygonize to form mosaic networks (Hanley et al. 1977; Sumida and Lang 1981). These networks are visible in CL (Fig. 15) due to their frequent association with a luminescent source known as Band-A emission (Hanley et al. 1977; Graham et al. 1991), and are the most commonly observed internal feature in Type IIa and IIb diamond (e.g., Smith et al. 2016b, 2018). The lack of any observable growth zones most likely relates to the lack of nitrogen-related defects in these diamonds, or otherwise to deformation overprinting any growth features. Regardless, the distinct defect characteristics of Type I and Type II diamonds means that there may be no necessity to invoke different external stress regimes in the mantle for the different internal patterns observed.

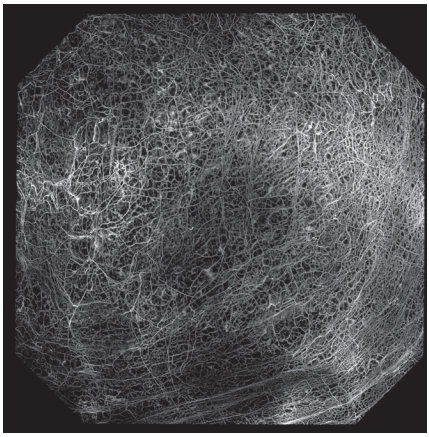

Figure 15. Cathodoluminescence image of a polygonized dislocation network on the table of a faceted Type IIb diamond. 4.8 mm × 4.8 mm. [Image by Karen Smit.]

Internal features of Type I (nitrogen-containing) diamonds

In the majority of diamonds, the growth of Type I single diamond octahedra and cubes is not continuous, but consists of distinct growth episodes. This growth zonation gives a distinct stratigraphy to the diamond when viewed on either (100) or (110) polished sections under CL. Diamonds are not normally examined on {111} surfaces because as a growth surface, no pattern may be seen and additionally {111} surfaces are difficult to polish. Perfect octahedral patterns from the crystal center to the edges are only rarely seen—for example in a Russian octahedron (Bulanova et al. 1999) and in an elongated octahedron from Ghana (Seal 1965) (Fig. 16).

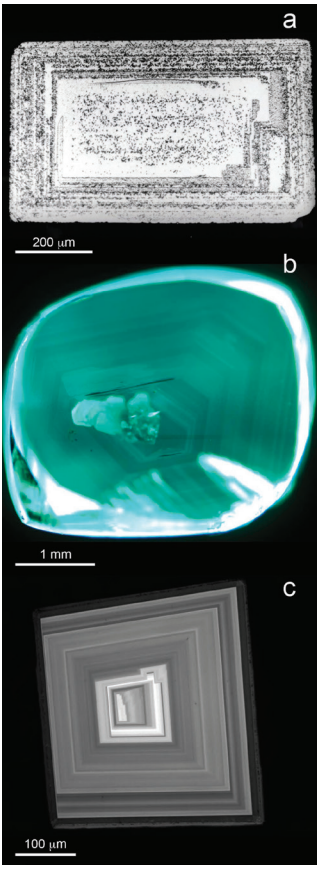

Figure 16. (**a**) Regular octahedral growth patterns observed in an etched (100) surface of a slightly elongate octahedral diamond from Ghana. (**b, c**) Regular octahedral growth patterns observed in CL images of diamonds from Ellendale (Australia) and Ekati (Canada). [Image in (a) reprinted from Seal (1965) with permission from the Mineralogical Society of America. Image in (b) from Smit (2008). Image in (c) from Zhang (2016).]

In some cases, growth zones that are visually distinct in CL between the core area and the periphery show sharp variations in isotopic characteristics. Such observations indicate that there have been at least two distinct and separate growth events and age dating of inclusions indicated that these different zones grew billions of years apart (Wiggers de Vries et al. 2013; Bulanova et al. 2014).

Not all Type I diamonds have a definable growth pattern. Figure 17 shows diamonds that have poorly defined central regions with structural order towards the edge. In the Bultfontein diamond, the central area might be part of a cuboid growth zone before octahedral surfaces developed. The darker growth zones, with a low CL response are thought to be Type II (low nitrogen) diamond.

Using X-ray topography, Moore and Lang (1972) studied diamonds of cubic habit and recognized two very distinct growth patterns—cuboid and fibrous. *Cuboid growth* (Fig. 18a) consists of a hill-and-valley structure (in the scientific literature variously described as 'hummocky', 'crinkly' or 'cobbled') of average orientation in one of the cube directions <100>. *Fibrous cubes* (Fig. 18b) have a fibrous (or 'columnar') internal structure, starting from the center of the stone and running, not in <100> directions, but in the <111> octahedral directions towards the cube corners. The sectors in between these principal directions are filled by branched fiber growth in four directions. The incorporation of impurities (which also causes the color) prevents the lateral growth of layers in the more usual {111} faceted growth, and only columns are formed (Moore and Lang 1972). The roughness of cube 'faces' arises from fiber-branching. For example, the (001) surface of the cube can be reached by taking steps parallel to [111], [$\bar{1}$11], [$\bar{1}\bar{1}$1] and [1$\bar{1}$1] in a multiplicity of paths of equal length. The cubic shape is a natural consequence of such growth. Some post-growth dissolution can cause the already-rough surface to be covered in square-shaped pyramidal pits called tetragons (Sutton 1928).

Figure 19 shows a diamond that exhibits partial cubic patterns, which are sometimes blocky and riddled with nitrogen-free Type II diamond. A principal conclusion after examining such complex surfaces is that we still have a lot to learn about how some diamonds grow. See also Figure 8.

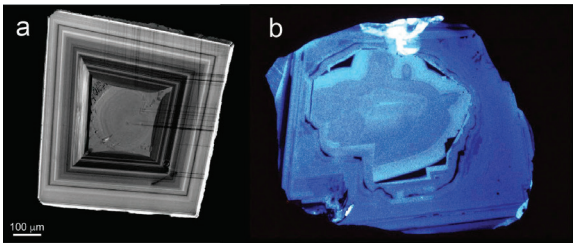

Figure 17. Cathodoluminescence images of diamonds that have poorly defined central regions with more orderly octahedral growth towards the edge. (**a**) Diamond from Grizzly kimberlite (Ekati mine) and (**b**) Diamond from Bultfontein (South Africa). [Image in (a) by Zhihai Zhang (Dalhousie University) and (b) by Jeff Harris.]

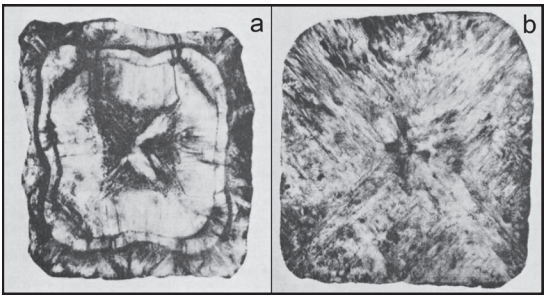

Figure 18. (**a**) Mid-section X-ray topograph of a colorless diamond cube of width 1.8 mm, showing truncated cuboid growth in its outermost regions. The growth rate of an octahedral face (top right) has been increased by dislocations, and consequently this face (or 'truncation') has grown out by the time it reaches the next visible outline. (**b**) Mid-section X-ray topograph of a brown diamond cube of width 1.9 mm, showing fibrous growth in <111> directions. [Figs 1 and 2a from Moreton Moore and A. R. Lang (1972) On the internal structure of natural diamonds of cubic habit, The Philosophical Magazine: A Journal of Theoretical Experimental and Applied Physics, 26:6, reprinted by permission of the publisher Taylor & Francis Ltd.]

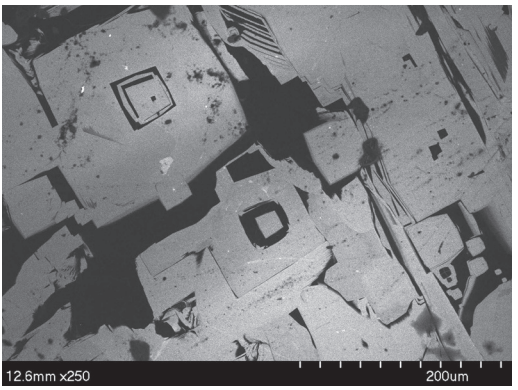

Figure 19. A (100) surface of a Bingara diamond (SE Australia) showing a complex but basically cuboid growth pattern, with Type I and Type II (dark) diamond intimately associated. [Image used with permission of Rondi Davies (Queensborough Community College, City University New York).]

Mixed-habit diamonds with cubo-octahedral growth

Harrison and Tolansky (1964) cut a clear 2.4 mm good quality, but slightly yellow, coated octahedron into eleven slices and etched them to examine in detail the growth history patterns of what became known as center-cross diamonds (Fig. 20). The center-cross pattern results from mixed-habit growth of flat octahedral planes and more hummocky cuboid surfaces (Lang 1979). The cuboid growth sectors in mixed-habit diamonds often contain tiny particles (1–5 μm), which if in sufficient concentration give rise to the visible petal arrays seen in some diamonds (Lang 1979; Rakovan et al. 2014). Cuboid zones often contain higher concentrations of nitrogen, nickel, hydrogen, methane and graphite (Bulanova et al. 2002; Lang et al. 2007; Rondeau et al. 2007; Howell et al. 2013; Smit et al. 2016b) (Fig. 21).

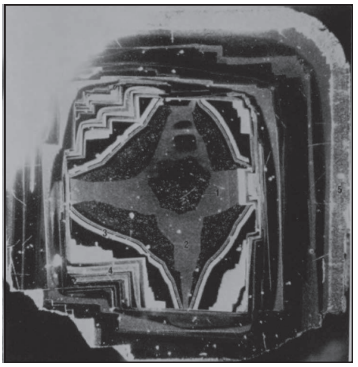

Figure 20. A clear 2.4 mm coated octahedron with an internal growth patterns of what became known as center-cross diamonds, now known as mixed-habit or cubo-octahedral diamonds. [Republished with permission of The Royal Society (U.K.), from Growth history of a natural octahedral diamond. Harrison ER, Tolansky S (1964) Proc R Soc London A 279:490–496; permission conveyed through Copyright Clearance Center, Inc.]

Mixed-habit diamonds can show a wide range of growth patterns that depend on whether cuboid or octahedral growth is dominant. Figure 22a shows a crystal developed from a cube core to an octahedral outer shape and Figure 22b the reverse, a possible controlling condition being mantle temperature. An example where directional growth is less perfect is shown in Figure 22c, giving rise to a repetitive pattern of cube or octahedral dominance. The mechanisms of how mixed-habit crystals can develop from a cubic core to an octahedral outer shape are detailed in Zedgenizov et al. (2006) and Howell et al. (2013).

There are only a limited number of studies on mixed-habit diamonds from specific locations. Welbourn et al. (1989) studied the variation of nitrogen content and other spectroscopic features between cuboid and octahedral sectors in mixed-habit Jwaneng diamonds. Bulanova (1995) and Bulanova et al. (2002) documented inclusion parageneses and carbon and nitrogen isotopic characteristics in mixed-habit Yakutian diamonds. Kaminsky and Khachatryan (2004) examined

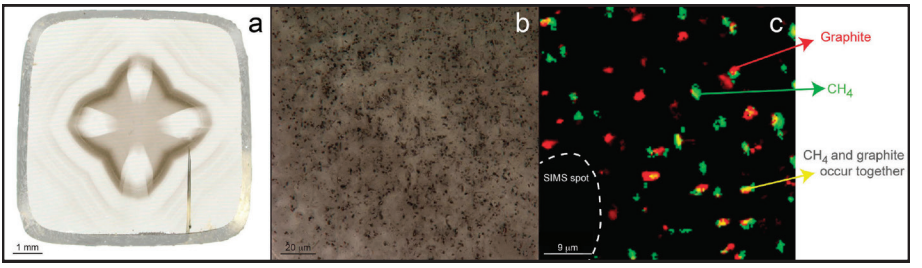

Figure 21. (**a,b**) In some cubo-octahedral diamonds, the cuboid sectors are visible in plain light because they often contain tiny micron-sized particles. (**c**) In Marange, and other diamonds of unknown origin, these particles have been identified as graphite by Raman spectroscopy (Howell et al. 2013; Smit et al. 2016b). [Images in (a,b) by Karen Smit. Raman map in (c) reprinted from Smit et al. (2016b).]

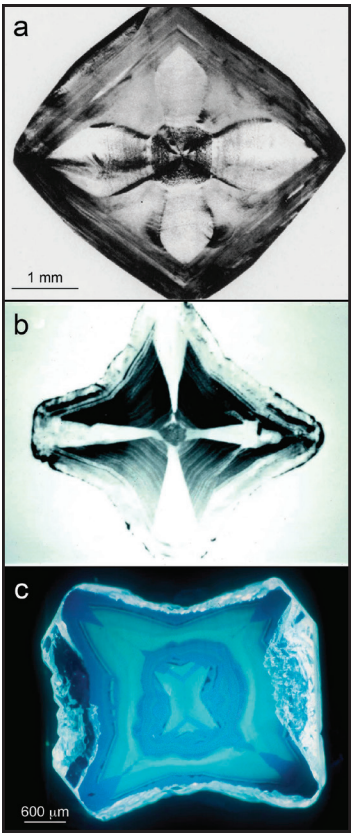

Figure 22. (**a**) Mixed-habit cubo-octahedral diamond in which there has been a smooth variation in ratio and rate of growth between cuboid surfaces and {111} faces. (**b**) A Jwaneng diamond (2–3 mm across) showing smooth variation between octahedral and cubic growth, resulting in a re-entrant cube. (**c**) A re-entrant Jwaneng cube showing repetition of octahedral and cuboid growth zones. [Image in (a) reproduced from Lang (1974b) with permission from Elsevier. Image in (b) reproduced from Welbourn et al. (1989) with permission from Elsevier. Image in (c) courtesy of De Beers.]

the variation of nitrogen content and aggregation state in Yakutian, Urals and Arkhangelsk mixed-habit diamonds. Davies et al. (2004) and Aulbach et al. (2009) both document cubo-octahedral diamonds in eclogitic and peridotitic diamonds from Lac de Gras (Canada). Smit et al. (2016b) studied mixed-habit diamonds from Marange (Zimbabwe), and used fluid inclusion content combined with isotopic characteristics of the diamonds to model diamond growth from hydrous fluids.

Features of Type Ib diamonds

Type Ib diamonds contain abundant neutrally charged isolated substitutional nitrogen (N_S^0, known as C centers) and account for less than 0.1% of natural diamonds (Harlow 1998), although this percentage is not well constrained. This rarity is because over geological time and at temperatures typical of the cratonic lithosphere, isolated nitrogen aggregates to A centers (N pairs) and B centers (4N around a vacancy). For further details on these and other defects in diamonds, see Green et al. (2022, this volume). Preservation of N_S^0 in natural diamonds is normally explained through either short mantle residency times or storage at $T < 700$ ºC (Taylor et al. 1996), whereas most cratonic diamonds are billions of years old and resided at $T > 1000$ ºC (Stachel and Harris 2008; Shirey and Richardson 2011).

Very few natural Type Ib diamonds contain 100% C centers, and the majority of these diamonds have undergone some aggregation to A centers. Aside from age and mantle temperature, the extent of Type Ib-IaA aggregation also depends on the amount of nitrogen initially incorporated into the diamond lattice during growth. If total nitrogen content is low, nitrogen aggregation may remain low since during annealing and diffusion, one nitrogen atom does not meet another.

In recent years, there have been several studies that document the internal features of rare natural Ib diamonds from French Guiana, eastern Sierra Leone, NE Siberia, and Botswana (Smith et al. 2016a; Zedgenizov et al. 2016; Smit et al. 2018b; Timmerman et al. 2018). These diamonds are mostly yellow-orange due to the presence of isolated nitrogen.

Diamonds recovered from highly altered rocks interpreted to be komatiites in French Guiana exhibit a mixture of growth signatures that are blocky, sectorial, granular or polycentric, and associated with intense plastic deformation (Fig. 23a,b; Smit et al. (2016b). At Zimmi (Sierra Leone), brownish- or greenish-yellow alluvial dodecahedroid-THH diamonds have complex internal patterns (Fig. 23c,d; Smit et al. (2018b). In part the diamond appears to be like a calving ice-sheet, the darker diamond being a second generation of diamond infiltrating the original. The origin of these patterns is unclear, although they do not appear to be related to *plastic deformation lines/planes* commonly seen in these diamonds.

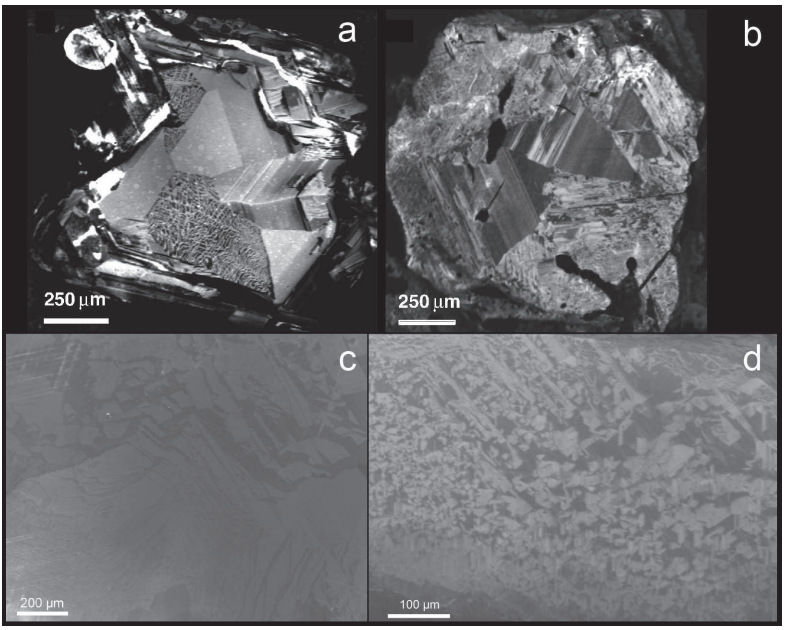

Figure 23. (**a**) and (**b**) Internal patterns of two Dachine Type Ib diamonds with blocky polycentric growth. (**c**) and (**d**) Internal patterns of unknown origin visible in CL images of Type Ib diamonds from Zimmi. [Images in (a, b) from Smith et al. (2016a) with permission from Elsevier. Images in (c,d) reprinted from Smit et al. (2018), Mineralogy and Petrology.]

Some cuboid alluvial diamonds from NE Siberia exhibit faint concentric growth patterns (Fig. 24; Zedgenizov et al. (2016), whereas other diamonds from this locality had heterogeneous patterns and high levels of plastic deformation. In some diamonds, growth zoning correlates with heterogeneous yellow color distribution. In Botswana, the Orapa mine has produced some irregular cubo-dodecahedral diamonds, with some color differences between the different growth sectors (Timmerman et al. 2018).

At typical mantle temperatures, the first stage of nitrogen aggregation in diamond (isolated nitrogen to nitrogen pairs) has been shown to occur very quickly (Taylor et al. 1996). Thus the preservation of Type Ib diamonds needs special geological environments shortly after their formation that are distinct to those of more common Type Ia diamonds. The presence of deformation features in Type Ib diamonds may indicate a rapid rise to cooler parts of the mantle (e.g., Smit et al. 2016a, 2018b), however this may not be true for all localities and

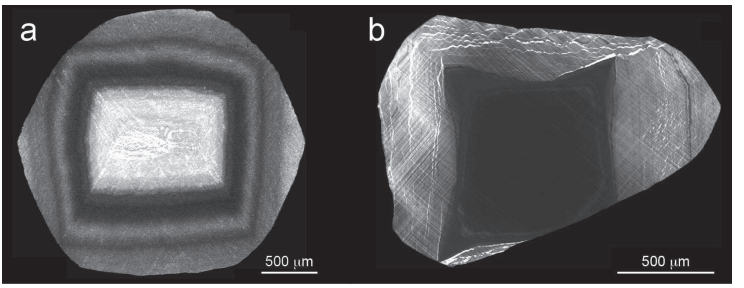

Figure 24. Cathodoluminesence images showing the growth patterns of cuboid alluvial diamonds from NE Siberia: (**a**) Dodecahedroid diamond with cuboid growth zones. (**b**) Rounded cuboid diamond with central cuboid domain. [Reprinted from Zedgenizov et al. (2016), with permission from Elsevier.]

Type Ib diamonds may also survive due to the diamonds' long residence in low temperature portions of the diamond stability field. Additionally, the Siberian diamonds could have formed close to the time of kimberlite eruption. One unifying aspect of these rare diamonds is that at present, they all belong to the eclogitic paragenesis.

Twinned diamonds

The internal growth structures for both contact and interpenetrant twins have been studied principally by X-ray topographic techniques (Machado et al. 1998; Yacoot et al. 1998). For contact twins, the twin plane was found not to be always planar but with twin interpenetrant components. As mentioned above, the initial contact twinning was shown to be nearly always at the center of the diamond and this was sometimes marked by a visible inclusion (Fig. 25). The second group consisted of fibrous diamonds. X-ray topographs of this type of crystal showed that fibrous growth is in octahedral directions (see Machado et al. 1998) occurring without the need of branching as happens with single fibrous cubes and again, nucleation was near the crystal center.

Figure 25d shows a section across a typical macle twin plane, one side of which exhibits a complex growth pattern, the other having no pattern at all. As this surface is generated by a potassium nitrate etch, the absence of a pattern would signify a Type II diamond adjacent to a Type I. Seal (1965) suggested that the stark difference may be due to crystal orientation effects. If that proposal should not be the case and Type I and II diamond exist across a twin plane, then some serious thinking about diamond formation is required.

Concluding remarks

Within the sizes of diamonds usually studied—microdiamonds up to 5 mm, with rare examples of larger stones—the main growth patterns of diamond have probably now been identified. A thorough understanding of the internal growth structure of a diamond—and core-to-rim growth directions—is important since the outward variation of carbon and nitrogen isotopes can sometimes be related to the redox conditions of the diamond source fluid.

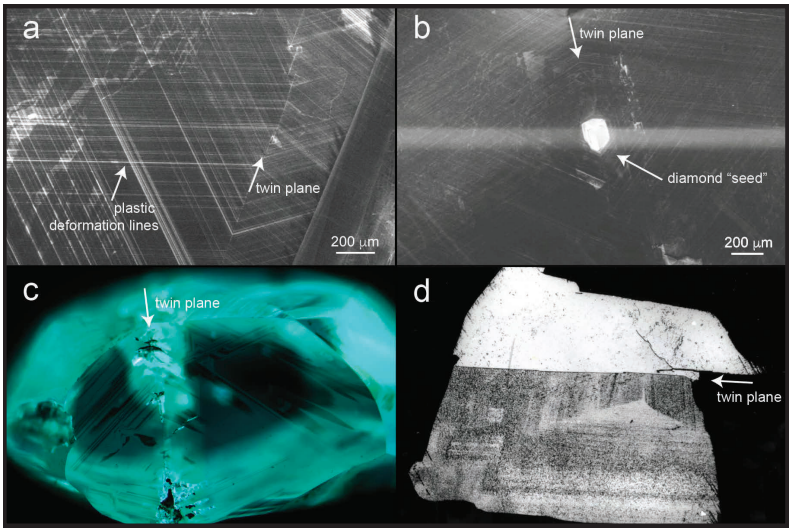

Figure 25. Examples of twin planes on the internal surfaces of diamonds: (**a**) Twin plane + plastic deformation lines. (**b**) Diamond inclusion visible along a twin plane in a Zimmi diamond. (**c**) Etching along a twin plane in an Ellendale diamond. (**d**) twinned diamond from Ghana (2 mm length) showing distinct growth characteristics either side of the twin plane. [Images in (a,b,c) by Karen Smit. Image in (d) reproduced from Seal (1965) with permission from the Mineralogical Society of America.]

SURFACE TEXTURES

The surface of natural diamond shows relief features of varying degrees of complexity, which are the result of either crystal growth or subsequent partial dissolution of growth layers during metasomatic events in the mantle and/or during transportation by the deep-seated mantle magmas (kimberlites and lamproites) to Earth's surface. Any post-emplacement alluvial history may add further traces of mechanical wear on diamond surfaces. The shapes of the surface features created during metasomatic events invariably reflect the crystal symmetry of the primary diamond shapes of octahedra and cubes (and their twin equivalents). In the case of the dissolved dodecahedroids and THHs, features are either crystallographically approximate to the symmetries of those crystals, or independent of such symmetry. With alluvial diamonds initial impact damage is not governed by crystallography, although the development of that damage may have a crystallographic component.

There is a great variety of surface textures observed on all the principal shapes of natural diamond. Some have a very common general occurrence whereas others are extremely rare. In almost any diamond population there are diamond crystals with unusual surface features, whose origins are still difficult to interpret. Many surface features have been reproduced in controlled experiments at high pressures and temperatures, providing constraints on the conditions of their formation within the Earth.

Linking surface features to growth or dissolution events in the mantle requires knowledge on (1) how to discriminate growth features from dissolution features, and (2) how to discriminate dissolution features formed during mantle metasomatism from those induced by interaction with kimberlite magma. Finally, as the surface features of micro-diamonds can be linked back to specific kimberlite lithologies and a depth interval within the kimberlite pipe, a better understanding of the relationship between diamond dissolution style and kimberlite type and lithology can be established. As surface features can also be reproduced in controlled experiments, these relationships help to reconstruct the emplacement mechanisms of different kimberlite bodies.

In this section we first describe features that are seen on diamonds from kimberlites or lamproites and then consider a similar assessment of alluvial diamonds.

Octahedral growth features

Perfectly shaped flat-faced sharp-edged octahedra are not common in most diamond productions. Invariably diamond growth is imperfect, which gives rise to three principal surface features: triangular plates, imbricated surfaces, and pyramids.

Triangular plates. These have an outline that follows the shape of diamond's octahedral face, can be single but are usually multiple, and with each consequent plate they decrease in size (Fig. 26). The thickness of the plates can vary but usually it is possible to clearly

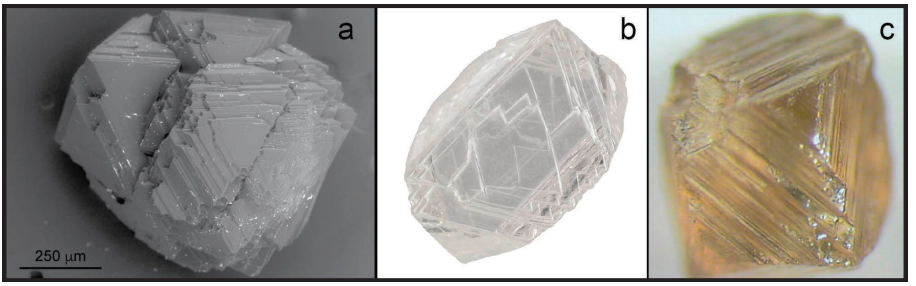

Figure 26. (**a**) Triangular plates on an Orapa diamond. (**b**) Triangular plates on a Diavik diamond (7.97 × 4.73 × 3.58 mm). (**c**) A striated octahedron (3 mm across) resulting from diminishing step growth. [Image in (a) by Yana Fedortchouk. Image in (b) by Jian Xin (Jae) Liao (GIA). Image in (c) by Jeff Harris.]

distinguish one step-face (plate) from another. The edges and corners of the growth step-faces can be sharp or slightly rounded by later dissolution. Diamonds with growth step-faces are fairly common. Experimental work by Yamaoka et al. (1977) shows that this growth shape is confined to a narrow growth region close to the diamond/graphite equilibrium line. The growth origin of these faces is evident from the stepped growth patterns on CL images of sections through the diamonds with this surface feature (Fig. 27).

Imbricated surfaces. If the incomplete growth of triangular plates prevents an octahedral vertex from forming and the edges of particular plates overlap, then the result is an *imbricated surface*. In some instances imbrication creates a pseudo-cube face made up of the triangular vertices of the plates (Fig. 28).

Pyramids. These are positive-relief triangles, with their base oriented parallel to the edges of the octahedral face and cover only part of an octahedral face. The more obvious pyramids develop at the octahedral vertices giving rise to a negative triangular depression in the middle of that face.

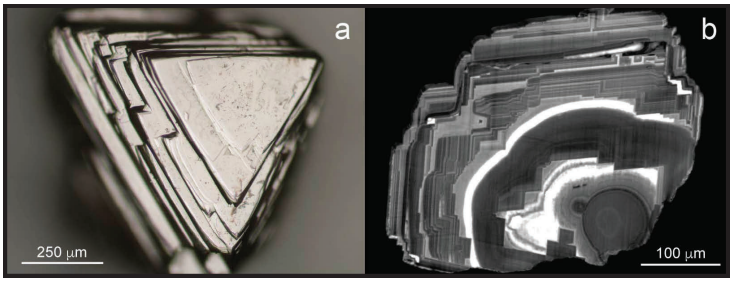

Figure 27. (**a**) An octahedral diamond from Misery (Ekati mine) showing well-defined thick triangular plates with straight sides and slight rounding due to dissolution. (**b**) CL image showing that triangular plates follow the stepped growth pattern of the diamond confirming their growth origin. [Image in (a) by Yana Fedortchouk. Image in (b) by Zhihai Zhang (Dalhousie University).]

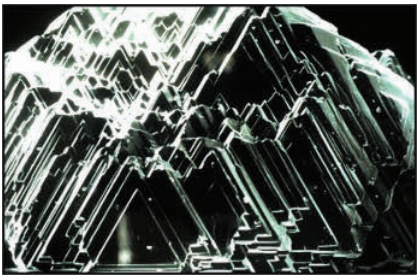

Figure 28. A South African octahedron exhibiting imbrication. [Image by Jeff Harris.]

Octahedral dissolution features

Dissolution features considered in this instance are those that are associated with major octahedral to dodecahedroid (or THH) conversion (Fig. 10), but dissolution still leaves a recognizable octahedral shape. These features also apply to primary octahedral macle surfaces.

Shield-shaped and serrate laminae are consequences of the dissolution of triangular plates on octahedral surfaces, or the octahedral surface itself. Dissolution commences at the corners and edges and moves across a face creating a triangular convex shape resembling a shield (Fig. 29). In the case of an octahedral face the shield is formed from the partial exposure

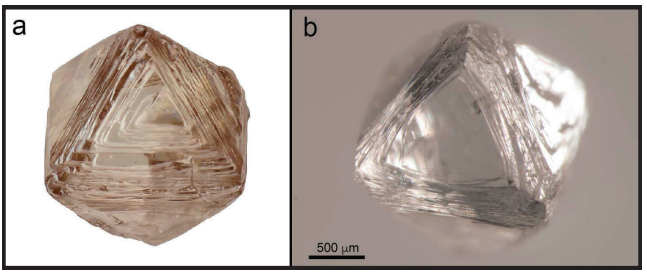

Figure 29. Shield-shaped laminae in octahedral diamonds from (**a**) Diavik (Canada) with 5.26 × 4.92 × 6.17 mm dimensions and (**b**) Koffiefontein (South Africa). [Image in (a) by Jian Xin (Jae) Liao (GIA). Image in (b) by Nicole Meyer (University of Alberta).]

of the original growth layers of the diamond. Serrate laminae only partially cover a face often having a zig-zag outline to their edges (Fig. 30). They result from dissolution of an imbricated surface or on diamonds with thin internal growth zoning at mantle conditions. They also often appear to be accompanied by numerous trigonal etch pits (see below). *Shield-shaped and serrate laminae* very similar in form to those found on natural diamonds have been produced at mantle pressures of 5–7 GPa during diamond dissolution experiments in silicate-carbonate melts (Khokhryakov and Pal'yanov 2007). Laminae shapes are influenced by variations in temperature and also amount of carbonate (Fedortchouk et al. 2019).

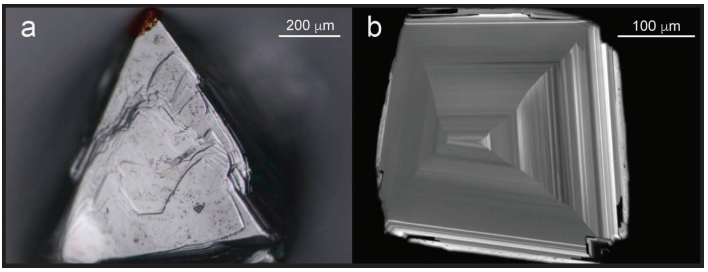

Figure 30. Octahedral diamond with serrate laminae caused by dissolution (Misery kimberlite, Ekati Mine). (**a**) Microphotograph showing serrate laminae. (**b**) Cathodoluminescence image showing thin growth zones, ideal for serrate laminae formation through dissolution. [Images by Zhihai Zhang (Dalhousie University).]

Trigons. Trigons are triangular features that are defined as being either 'positive' or 'negative' (Frank et al. 1958). A positive trigon has the same orientation as the triangular octahedral face of the diamond; whereas a negative trigon has the opposite orientation.

Negative trigons are a very common feature on octahedral surfaces. They can vary in size, depth and shape, even on the same diamond. Trigons range from about 5 μm in diameter to ~100 μm. Two principal trigon morphologies can be distinguished (1) plain flat-bottomed (f/b) trigons (Fig. 31a,b) and (2) deeper stepped-faced and point-bottomed (p/b) trigons (Fig. 31c,d) that are sometimes associated with hexagons (see below). Flat-bottomed trigons have even been observed on diamonds recovered from inside an eclogite xenolith (Larry Taylor, pers. comm.) When f/b and p/b trigons occur on the same diamond, they are typically grouped by size ranges. In some kimberlites, diamonds with small f/b trigons (less than about 5 μm in diameter) evolve into p/b as they grow larger whereas in other kimberlites the opposite trend is noted (Fedortchouk 2015 and unpublished data). Also, f/b and p/b trigons have different relationships between their diameter and depth. For example, on the same diamond f/b trigons often have similar diameters but a large range of depths, whereas p/b trigons show a strong positive correlation between their diameter and their depth (Fedortchouk 2015).

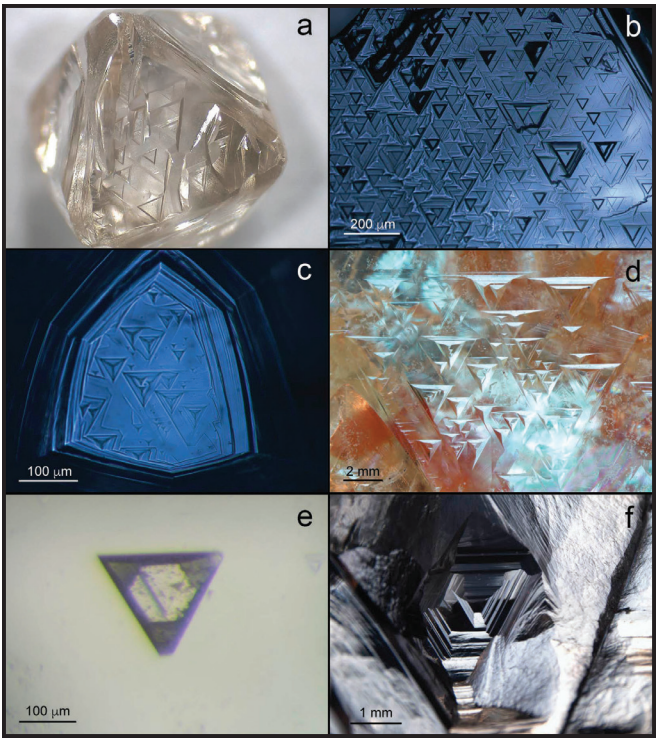

Figure 31. Negative trigons. (**a,b**) Flat-bottomed (f/b) trigons on diamonds from Gahcho Kué and Snap Lake. (**c,d**) Point-bottomed (p/b) trigons on a Misery kimberlitic diamond and Sierra Leone alluvial diamond. (**e,f**) Truncated trigons combining walls of positive and negative orientation (Orapa cluster AK15 and Letšeng). [Images in (a,b) courtesy of Ingrid Chinn (De Beers Exploration). Images in (c,e) by Yana Fedortchouk. Images in (d,f) by Evan Smith (GIA).]

Experiments conducted at 1–3 GPa and 1150–1350°C suggest that higher CO_2 content in kimberlitic fluids correlates with (1) increasing size and abundance of p/b trigons at the expense of f/b trigons (Fedortchouk 2015; Zhang et al. 2015) and also (2) the development of positively-oriented walls inside negative trigons (resulting in truncated trigons).

Their formation on octahedral surfaces often seems random, but Lang (1964) and Frank and Lang (1965) established by X-ray topography that point-bottomed (pyramidal) negative trigons were etch-pits resulting from preferential removal of material from locations where dislocations outcropped on the external surface of the crystal. Frank and Lang (1965) recorded that no dislocations outcrop beneath flat-bottomed trigons. For the theoretical grounds explaining the association of point- and flat-bottomed etch pits on minerals with different types of defects see Lüttge (2006). Sometimes lines of negative trigons are observed running across octahedral faces parallel to octahedral edges, and trigon development exploits the weakness created at the surface by *plastic deformation lines/planes*.

Positive trigons are very rare on octahedral surfaces of natural diamond and are usually found only on the smallest sized stones. At Snap Lake (Canada), positive trigons were found on microdiamonds of size ≤ 300 μm to 1.7 mm (Li et al. 2018). During diamond classification studies by Harris in the 1970s (unpublished data), *positive trigons* were seen in the ~1 mm-sized diamonds from Finsch (South Africa). As present-day cut-offs for diamond recovery are now usually set at ~2 mm, diamonds showing this surface feature have probably become particularly rare. In addition, at the Ekati kimberlite cluster (Canada) *positive trigons* occur

on microdiamonds recovered from coherent hypabyssal kimberlite in the Grizzly pipe but are lacking on microdiamonds from volcaniclastic kimberlites (Yana Fedortchouk, unpublished data). Thus, it may be that positive trigons are a feature of diamond dissolution in hypabyssal conditions, where high-temperature fluids are present at near-surface pressures.

Figure 32 shows f/b positive trigons on a Finsch mine diamond and one from Snap Lake. Those from Finsch have edges of ~20 μm whilst Snap Lake edges are 1–3 μm. At both localities *positive trigons* overprint earlier dissolution features such as f/b negative trigons and may not be evenly distributed over an octahedral face. At Snap Lake some very small positive trigons were found on the rounded edges of octahedra (Fig. 6a in Li et al. 2018). In South Africa this trigon type has also been noted with two other rare surface features known as *transverse hillocks* and *imbricate wedges* (Robinson 1979) (see Fig. 1c,d in Li et al. 2018). Experiments show that low pressure, high oxygen fugacity (fO_2), and fluid with > 90 mol% of CO_2 promote positive trigon development (Evans and Sauter 1961; Yamaoka et al. 1980; Zhang 2016). These conditions suggest that etching took place after kimberlite emplacement, representing very late-stage dissolution by kimberlitic volatiles.

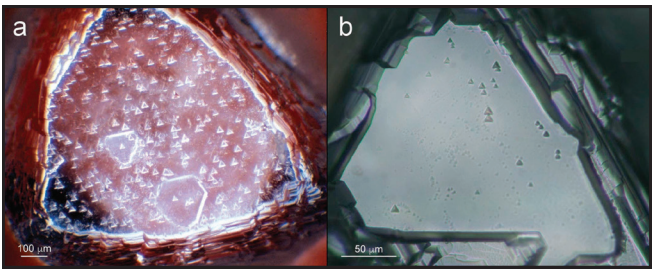

Figure 32. (**a**) A Finsch octahedron exhibiting positive flat-bottomed trigons in part overprinting earlier larger flat-bottomed truncated negative trigons. (**b**) Flat-bottomed (f/b) positive trigons on a Snap Lake diamond. [Image in (a) by Jeff Harris. Image in (b) by Yana Fedortchouk.]

Hexagons are six-sided pits that develop on octahedral faces and combine the components of positive and negative trigons (Fig. 33). Negatively oriented walls are steeper and flatter than those with positive orientation, which are shallower and show *striations*, *tetragonal or circular pits.* Hexagons are usually larger and deeper than trigons, their base being flat or rugged, the former often having *small trigons* on the bottom. *Hexagons* are less common than *trigons*, but diamond populations from almost any kimberlite have some of this type of mantle dissolution. They were relatively common on diamonds in hypabyssal kimberlite from Snap Lake (Li et al. 2018) and the lamproitic Argyle Mine in Western Australia (Hall and Smith 1985). Figure 33a shows a typical diamond with hexagons from Argyle.

As negative and positive trigons have been shown to be two separate dissolution events, the formation of hexagons is most likely the result of dissolution conditions being close to the boundary region for these dissolution mechanisms. At Snap Lake this relationship was studied at the 1–10 μm scale (Li et al. 2018) where there appeared to be an association, positive trigons developing inside negative pits making them hexagons (Fig. 33d). Experiments indicate that the larger hexagon formation is promoted by high CO_2 content (> 90 mol%) of magmatic fluid (Fedortchouk et al. 2007; Zhang 2016) and by dissolution in carbonate melts (Fedortchouk et al. 2019).

Cubic growth features

Flat-faced sharp-edged gem quality cube diamonds are much more rare than octahedra with equivalent characteristics. Perhaps the nearest to cube perfection are some of the diamonds from Wawa in Canada (see Fig. 2 in Stachel et al. 2006).

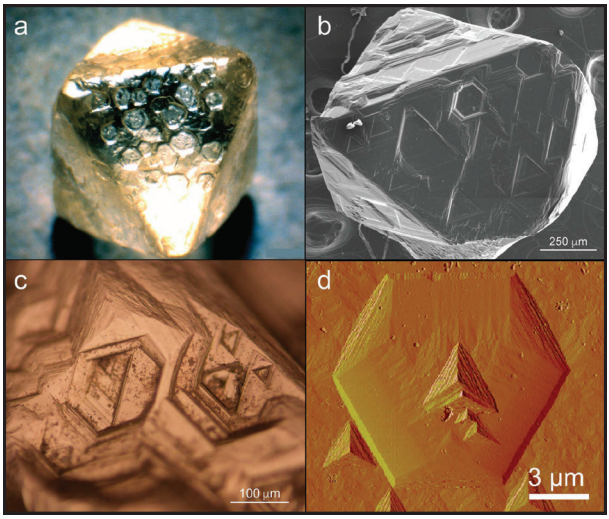

Figure 33. (**a**) A 5 mm Argyle octahedron exhibiting hexagons, a common surface feature of Argyle diamonds (Australia). Hexagons on diamonds from (**b,c**) Leslie kimberlite, Ekati Mine (Canada) and (d) Snap Lake Mine (Canada). [Image in (a) reprinted from Hall and Smith (1984) with permission from the University of Western Australia. Images in (b–d) by Yana Fedortchouk.]

The original growth of the larger gem diamonds may have created the smooth hummocky surfaces observed, but the association with tetragons (see below), probably indicates that original growth features have been modified or obliterated by dissolution. The smaller and more regular gem and opaque flat-faced cube diamonds have surfaces which are finely pock-marked, but whether or not this is a growth feature is uncertain.

Cubic dissolution features

Dissolution causes the rounding of cube edges creating a small modification to the original shape. Cubic dissolution features however are not constrained only to diamond cubes. They can also develop on any {100} plane exposed to dissolution (e.g., an octahedron broken along a (001) plane with tetragonal pits and tetragons on that surface—Tom McCandless, pers. comm.).

Development of a single face along the cubic edge transforms cubes towards dodecahedroids while development of two faces one on either side of the original edge results in THH morphology (Khokhryakov and Pal'yanov 2007). These authors also show through dissolution experiments that transformation of diamond cubes into THHs requires twice the weight loss than octahedral transformations. The other very obvious and dominant cubic feature comprises crystallographically controlled etching consisting of tetragons, a feature like trigons, whose orientation is dependent on temperature and fO_2 (Fedortchouk et al. 2009).

Tetragons are tetragonal pits set at 45° to the cube edge (in the case of the usual negative tetragons) and which may cover all {100} faces (Fig. 34). The surfaces of some coated cubes from the Democratic Republic of the Congo have distinct, but incomplete cube patterns which parallel the cube edges. Whether this observation indicates an irregular growth of the diamond coat or a subsequent partial dissolution is uncertain (Jeff Harris, unpublished data).

In an extensive study of South African diamonds only one was found to have positive tetragons (with sides parallel to the cube edges) (Robinson 1979). Small *tetragons* may appear on four-fold surfaces of other diamond crystals, at crystal apices and positively oriented walls of hexagonal pits. The tetragon base can be deep point-bottomed or very shallow flat-bottomed

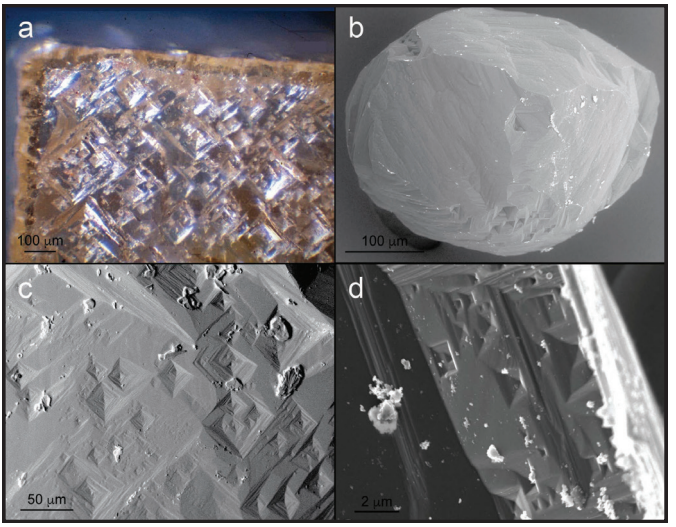

Figure 34. (**a**) Tetragons set in the negative orientation covering the whole of a cube face on a diamond from the DRC. (**b,c**) Dodecahedral diamond showing trigon dissolution pits in [111] direction (centre of the crystal) and point-bottomed (p/b) tetragons in [100] direction (upper left and lower areas of the crystal). (**d**) Small point-bottomed (p/b) tetragons formed on positively-oriented walls of hexagonal pits. [Image in (a) by Jeff Harris. Images in (b–d) by Yana Fedortchouk.]

and both types usually show terraced (stepped) walls. Robinson (1979) suggested that tetragon pits could represent the incipient forms of the *circular pits* sometimes found on diamonds and formed during late stages of dissolution by kimberlitic fluid.

Dodecahedroid and THH features

Two main surface features develop during dissolution of diamond octahedra to dodecahedroids and THHs, during ascent in kimberlite/lamproite magma: (1) low relief features and *plastic deformation lines/planes* linked to diamond crystallography, and (2) features which are independent of crystallographic control.

Low-relief features. The curved surface of a dodecahedroid face is sometimes smooth, featureless and glossy, but more commonly consists of an overall or partial *terracing.* The terraces arise because dissolution exposes the intermittent growth layers of the original octahedral surfaces, where terrace shapes are centered around <111> directions (Fig. 35).

Commonly associated with terracing are *hillocks*, which form on individual dodecahedroid surfaces normally elongated parallel to the long diagonal of the face. *Hillocks* can form as isolated features, but usually occur in groups or cover all faces of a diamond crystal. *Hillocks* form a complete array of shapes from smooth drop-shaped to pyramidal with relatively sharp and pointy apices. Their clear link to diamond crystallography can be seen, for example, through their alignment around three-fold axes and the way they radiate from four-fold axes (Fig. 36). Observational evidence indicates that there is a general uniformity of hillock type on dodecahedroid diamonds from the same kimberlite phase. This infers that the dissolution conditions in kimberlite magmas are the determining factor for hillock shape (Fedortchouk et al. 2017), however, in some cases, hillock shape could be influenced by minor cuboid growth and plastic deformation (Ingrid Chinn pers. comm.). A study of diamond plates cut through dodecahedroid diamonds from Udachnaya and Yubileynaya (Yakutia) showed that there was a strong association between hillock development and areas of intense plastic deformation (Khokhryakov and Pal'yanov 2009).

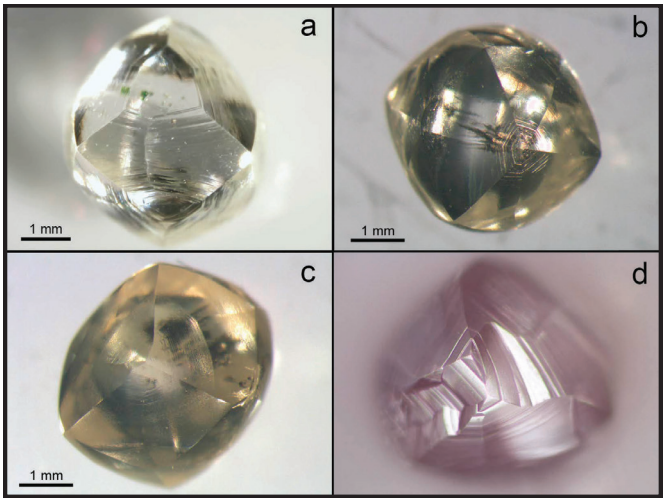

Figure 35. Examples of terraces on THH diamonds from volcaniclastic kimberlites. [Images in (a,b,c) by Karen Smit. Image in (d) by Yana Fedortchouk.]

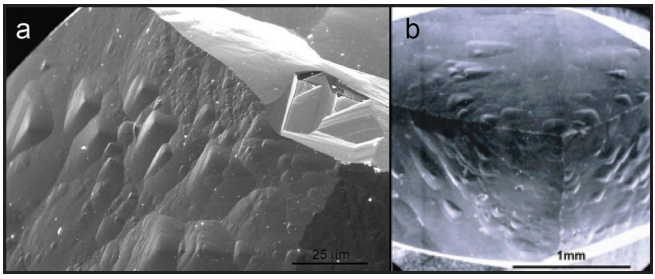

Figure 36. Hillocks are linked to diamond crystallography: in their alignment around three-fold axes, and the way they radiate from four-fold axes. [Image in (a) by Yana Fedortchouk. Image in (b) reproduced from Robinson (1979) with permission from the author.]

These low relief features have been reproduced in dissolution experiments in the presence of C–O–H fluid at 1 GPa and 1250–1350 °C (Kozai and Arima 2005; Fedortchouk et al. 2007) and often have a dominating presence in microdiamond populations from volcaniclastic facies kimberlite (Fedortchouk et al. 2017) both of which suggest that they develop when diamonds are carried by volatile-rich kimberlite magmas.

Plastic deformation lines/planes. The presence of variably spaced lines/planes running across a diamond (Fig. 37) is evidence that the diamond has been plastically deformed along its cleavage planes during residence at high temperatures in the mantle. The conditions for the transition from brittle to ductile (plastic) deformation in diamond shows that above 1000 °C, and in the pressure range expected for the sub-continental lithospheric mantle (1 to 6 GPa), ductile behavior is not very dependent on pressure (DeVries 1975).

More than one of the four equivalent sets of {111} cleavage planes may be involved when a diamond is plastically deformed. In these cases, the intersections of the *plastic deformation lines/planes* sometimes give rise to a *shagreen texture* over the dodecahedroid surface. Although this feature can be recognized on octahedral diamonds (see above), they

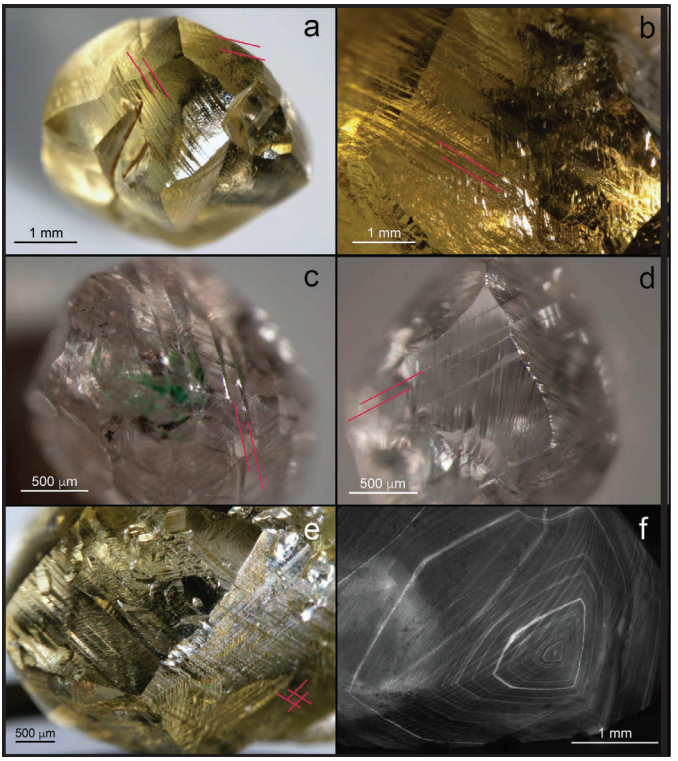

Figure 37. Plastic deformation lines/planes, indicated with **red lines** for clarity in (**a**) to (**e**). (**f**) Cathodoluminescence image that shows bright defects decorating the octahedral planes along which deformation occurred. [Images in (a,b,e,f) by Karen Smit. Images in (c,d) by Nicole Meyer (University of Alberta).]

are described here because diamond dissolution enhances the visibility of *deformation lines/planes* on dodecahedroid surfaces. The appearance of deformation lines/planes is variable, and can appear wavy (e.g., Argyle diamonds) or as straight planes through the diamond; and this distinction is probably due to differences in nitrogen content and aggregation state (Gaillou et al. 2010, 2012; Howell et al. 2015). Straight *deformation lines/planes* in 'non-Argyle-type' pink diamonds have been found to be due to deformation micro-twinning (Mineeva et al. 2007; Gaillou et al. 2010; Titkov et al. 2012).

The terms *lamination line* and *deformation lamellae* are also used to describe this surface feature, and to a lesser extent, *glide planes, slip planes* or *graining*. Historically, they were also known as *Tanganyika lines* because of their common occurrence in diamonds from the Williamson mine in Tanzania.

A measure of the proportion of diamonds deformed in a particular size fraction in a general diamond production can be gained by assessing the proportion of pink and brown diamonds present, as these colors are linked to plastic deformation (Collins 1982; Harris et al. 1983; Robinson et al. 1986; Fisher et al. 2009; Gaillou et al. 2010, 2012; Titkov et al. 2012; Howell et al. 2015). Not all deformed diamonds are brown, however, and experiments indicate that the color can be annealed out leaving just the deformation lines (Moses et al. 1999; Collins et al. 2000) a process that can occur naturally during high temperature storage in the mantle. For further details on the relationship between plastic deformation and pink and brown coloration in diamonds see Green et al. (2022, this volume).

Non-crystallographic features. *Corrosion sculpture* occurs on dodecahedroid surfaces as individual cavities of ~50 μm depth which are elliptical to irregular in shape with maximum diameters from 50 to 300 μm (Fig. 38a,b). The bases of the cavities are either smooth or striated and the cavities usually cover all the faces and edges of a crystal. *Shallow depressions* are generally restricted to dodecahedroid surfaces. These are equally irregular but larger in area, much shallower, and tend to occur in clusters. They are noticeable because they give a light frosting to the diamond surface (Fig. 38c).

Robinson et al. (1986) showed that in the 2.9 to 3.4 mm diamond size range for the major South African mines, high proportions of *corrosion sculpture* in a production were often matched by a smaller but significant proportion of *shallow depressions*, which might suggest similar conditions for their formation. Additionally, at the Wesselton mine in South Africa this relationship was kimberlite specific.

A more recent study by Fedortchouk et al. (2017) of 1 to 4.5 mm diamonds from the BK1 kimberlite (Orapa cluster) showed that *corrosion sculptures* were abundant in hypabyssal facies; and *shallow depressions* on diamonds in transitional partially fragmented hypabyssal facies. *Corrosion sculptures* are common on 1 to 3.5 mm diamonds in hypabyssal Gahcho Kué kimberlite, Northwest Territories, Canada (1 to 3.5 mm diamond size: Ingrid Chinn, pers. comm.). Experimentally, corrosion features and cavities develop on diamonds in volatile-undersaturated alkaline basalt, synthetic kimberlite, and carbonate melts at $P < 3$ GPa (Kozai and Arima 2005; Fedortchouk et al. 2007; Arima and Kozai 2008), but are not reported at pressures between 5 and 7 GPa (Khokhryakov and Pal'yanov 2007, 2010; Fedortchouk et al. 2019). Thus their occurrence in hypabyssal kimberlite and volatile-undersaturated experiments suggest an origin in kimberlite magma that did not exsolve a fluid phase.

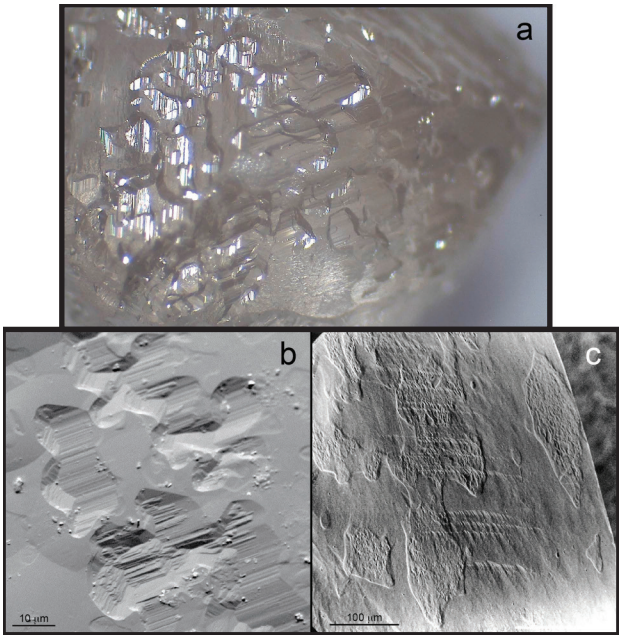

Figure 38. Examples of corrosive features on diamonds from hypabyssal kimberlites. (**a**) Corrosion sculpture on diamond from Gahcho Kué. (**b**) Corrosion sculpture on diamond from the Orapa kimberlite cluster. (**c**) Shallow depression on a South African diamond. [Image in (a) courtesy of Ingrid Chinn (De Beers Exploration). Image in (b) by Yana Fedortchouk. Image in (c) reprinted from Robinson (1979) with permission from the author.]

The occurrence of *frosting* on South African diamond productions was also investigated by Robinson et al. (1986) who divided this surface feature into coarse and fine frosting and showed the particular nature to be specific to the kimberlite source. Frosting on South African diamonds consisted of minute hexagonal to prismatic pits and occurred principally on dodecahedroids, but occasionally on octahedral diamonds. The frosting covered entire faces or only certain areas forming patches or islands. Examination of small to microdiamonds from Canadian productions (Fedortchouk et al. 2010) found the frosting to consist principally of micro-hillocks, which were either smooth drop-shaped (Fig. 39a) or sharp and pointy (Fig. 39b). Dodecahedroids with "smooth" *frosting* were common for all types of volcaniclastic kimberlite facies whereas those with "sharp" features occurred in hypabyssal kimberlites (Fedortchouk et al. 2010). Both authors considered this feature to be a very late-stage. Note that the general arrangement and the nature of *frosting* on diamonds in kimberlite is distinct from that caused by diamonds abraded in the alluvial environment (see below).

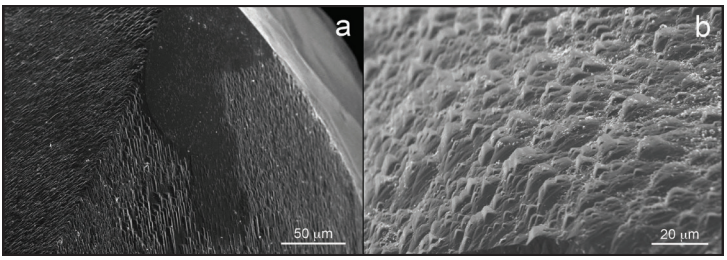

Figure 39. Secondary electron images of (**a**) frosting made of micro-hillocks with a smooth drop-like shape and (**b**) frosting made of sharp and pointy micro-hillocks. [Images by Yana Fedortchouk.]

Micro-disks are very minutely raised circular features on dodecahedroids and are described by Pandeya and Tolansky (1961), who proposed that the disks originated from an attachment of small fluid bubbles to the surface, momentarily protecting it from etching and leaving a raised disk behind. There is concentricity to some disks but others are more elliptical and curvilinear. The size of *micro-disks* is variable (Fig. 40). The disks overprint development of *terraces* and *hillocks,* and sometimes cover broken crystal surfaces indicating their origin during late-stage dissolution in kimberlite. The above authors also found an association with circular patterns known as *micro-pits*. Scanning electron microscope (SEM) images by Robinson (1979) showed these *micro-pits* to be nearly rectangular and about 10 μm in size. Microdiamond studies from the Ekati kimberlite mine identified two types of pit: one drop-shaped and the other with pyramidal walls (Zhang 2016) (Fig. 41). These *micro-pits* were found only on diamonds from volcaniclastic kimberlites where distribution varied from being present only on broken diamond surfaces in Panda and Koala pipes and occurring on dodecahedroid surfaces on diamonds from Misery and Fox pipes. In contrast, diamonds recovered from hypabyssal kimberlites (Leslie and Grizzly) did not display any *micro-pits*.

The limited experimental data on the formation of circular *micro-pits* reveal that they form in H_2O fluid at low pressure ($\leq$ 1 GPa), whereas addition of CO_2, dissolved SiO_2 and higher pressures suppress their development (Zhang et al. 2015). This could potentially make *micro-pits* (circular or other shapes) useful for deciphering conditions in kimberlite magma at the late stages of emplacement.

Ruts occur across some diamond surfaces and are of variable length, may be straight or sinuous, or may bifurcate (Fig. 42). According to Robinson (1979) the sides may be conspicuously etched and frosting sometimes extends into the rut. They are probably the result of weaknesses or pre-existing cracks being widened by an etchant passing between the diamond and its kimberlite matrix.

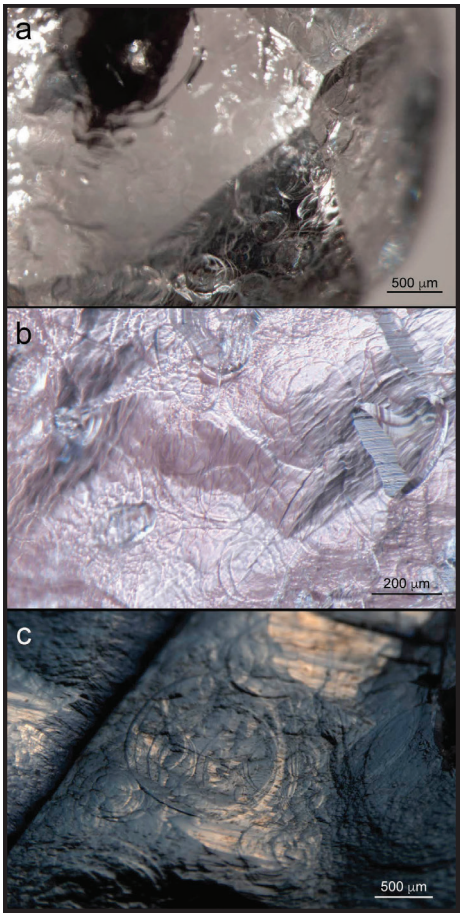

Figure 40. Examples of micro-disks on dodecahedroid and tetrahexahedroid surfaces. (**a**) Diamond from Koffiefontein (South Africa). (**b**) Diamond from Williamson (Tanzania). (**c**) Diamond from Letšeng (Lesotho). [Image in (a) by Nicole Meyer (University of Alberta). Images in (b,c) by Evan Smith (GIA).]

Rare surface features called *etch channels* or *spicules* are specifically considered by Lu et al. (2001) as hollow tubes open to the surface, ranging in form from straight to irregular and wormlike, some being interconnected and others showing crystallographic orientation. The openings have rhombic or modified rhombic shapes, widths of ~20–100 μm, lengths of ~200 μm–1 mm, and often terminate at solid inclusions. They occur in Type I and Type II diamonds and have a global distribution (Africa, Russia, South America, Australia and Canada) (Lu et al. 2001). *Etch channels* most likely originate from structural weaknesses on the diamond surface, such as dislocation bundles or where the edges of resorbed diamond intergrowths allow diamond dissolution to preferentially occur (Fig. 42a). These have then been aggressively etched and as dissolution proceeds, internal defects have either changed the direction or caused it to terminate, or the etching fluid has been depleted.

Surface features formed at the Earth's surface

Once diamond has been eroded out of its primary host rock, the new alluvial environment can cause additional surface features. These can be in the form of damage which overprints earlier characteristics, or surface color staining that is a consequence of radioactive bombardment. In the first case the damage can be very noticeable, affecting any diamond surface and can be found on all diamond shapes and most sizes, except the smaller stones (1–2 mm).

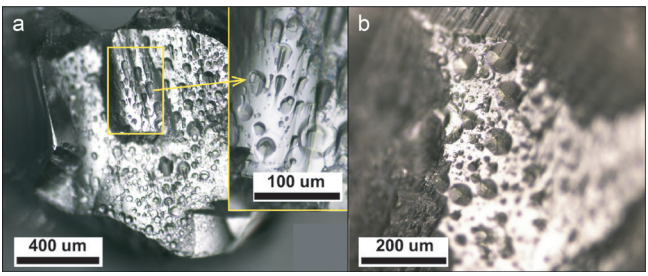

Figure 41. (**a**) Drop-shaped circular pits. (**b**) Pyramidal pits (transitional to tetragons). [Images by Zhihai Zhang (Dalhousie University).]

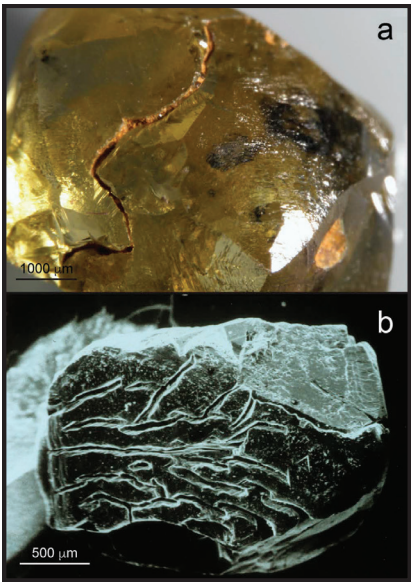

Figure 42. Ruts on diamond surfaces can be of variable length and shape, and result from fluid etching. (**a**) Diamond from Zimmi (Sierra Leone). (**b**) Secondary electron image of a Cullinan diamond exhibiting ruts across its octahedral surface. [Image in (a) by Karen Smit. Image in (b) by Jeff Harris.]

Radioactive damage can occur during diamond residence in primary kimberlite/lamproite after eruption, and/or more commonly in subsequent alluvial rocks. All shapes, surfaces and in this case, sizes can be affected. When irradiated in the primary kimberlite/lamproite, diamonds often have a totally transparent green coating. When irradiated in alluvial rocks, radiation damage is often observed as irregular and often localized green spotting. An exception is the diamonds in the Witwatersrand conglomerates that have a transparent green coating in addition to green radiation stains. Green radiation damage can turn brown if the diamond is heated above 600 °C (*discussed in more detail below*).

Alluvial surface damage. With diamond being the hardest known mineral, to be considering damage may seem superfluous, but diamond has a serious weakness in the form of a perfect cleavage. Such planes cause diamond to have a low brittle fracture. Thus, even if struck forcefully with an object less hard it may break along the {111} cleavage planes, whereas if progressively and slowly compressed the diamond will penetrate into the jaws of the press. In an alluvial environment, therefore, diamond can be damaged by local impacts or abraded during river transport. However, the probability of two diamonds colliding and causing damage to one another is extremely remote as the grade for alluvium is usually very low at about 1–2 carats per hundred tons. This diamond grade equates to one part diamond in 4.5×10^8 parts of rock.

The first sign of wear is abrasion damage to the *crystal vertices* and *crystal edges* particularly of octahedra, macles and dodecahedroids. Cubic diamonds would suffer the same fate except that many are either of poor quality and therefore do not survive transport, or if of gem quality are initially so exceptionally rare that damage has not been reported from an alluvial environment. The type of damage consists of very small breakages at the points and edges of the crystal (Fig. 43). If the *medial lines* of dodecahedroids are prominent or abrasion is relatively severe, then those edges may also be affected.

Impact damage takes the form of *percussion marks*, *chattermarks*, and *irregular surface scratches* (Fig. 44). In the case of *percussion marks*, the impact imparts an arcuate shape on the diamond surface, but directly within the diamond an internal fracture is created along the nearest cleavage plane to varying depths (micron scale). The size of this feature depends on the size and force of the impactor. *Chattermarks* are the result of a trail of closely spaced percussion marks whereas irregular surface scratches are aptly named random scratch-like marks on a diamond surface. The patterns of all these features can be quite varied.

A more structured alluvial abrasion feature which can be associated with those previously mentioned is a *network pattern*. The typical example shown in Figure 45 consists of two sets of {111} planes set at 109.5° apart. This configuration indicates they are probably the surface expression of two sets of plastic deformation lines/planes that were enhanced by abrasion. Finally, if a diamond becomes trapped, for example in an active pot-hole in a river course, mechanical wear may create a partial or all-over *frosting* giving the diamond a very dull appearance (Fig. 46).

Figure 43. An alluvial diamond from the Urals (Russia) showing abrasion of the edges of a tetrahexahedroid with lesser damage along the medial lines. [Image by Jeff Harris.]

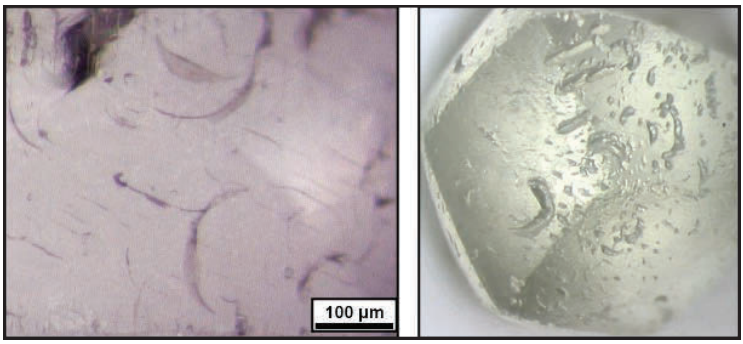

Figure 44. (**a**) Selection of different sized percussion marks on an alluvial diamond from the Urals (Russia). Note in the upper part of the picture, how the original percussion internally damages the diamond along a cleavage plane. (**b**) A 2–3 mm alluvial diamond from Namibia exhibits weak chattermarks with other irregular features of alluvial damage. [Images by Jeff Harris.]

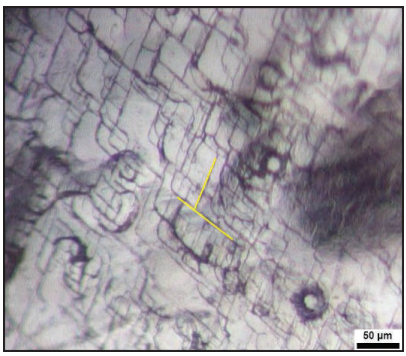

Figure 45. A diamond from the Urals (Russia) exhibiting a network pattern. [Image by Jeff Harris.]

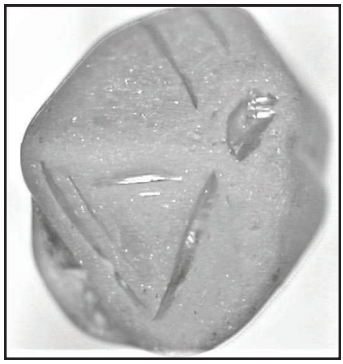

Figure 46. A 2–3 mm alluvial diamond from Namaqualand (South Africa) exhibiting heavy frosting due to abrasion. [Image courtesy of De Beers Exploration.]

Green radiation stains. Radioactive damage and the resulting color—occurring either during diamond residence in post eruption primary rock (kimberlite/lamproite) or in subsequent alluvium—is the result of persistent surface bombardment of α-particles, which have a penetration depth of up to 30 μm (Nasdala et al. 2013). During penetration the α-particle has sufficient energy to displace a carbon atom in the diamond lattice causing an atomic vacancy, thereafter losing its energy and becoming a helium atom. Diamonds with lower nitrogen content may be more likely to be damaged by radiation, as vacancy concentration has been shown to correlate with nitrogen content (Kiflawi et al. 2007). The created vacancy (GR1) is a color center and if there is sufficient concentration of GR1, visible green coloration results. The time taken for the color to be seen depends on the intensity of the radiation and may vary between 10 million years for uraninite contact (Vance and Milledge 1972) to around one billion years for the radioactivity in zircons (Nasdala et al. 2013).

Kimberlites have low concentrations of radioactive uranium and thorium (ppm range; Mitchell 1986) and therefore are only able to impart limited radiation damage to diamonds while they are still *in situ*. Nevertheless, the majority of transparent green-coated diamonds (Fig. 47) are found only in kimberlites. They are confined to the upper weathered portion of the pipe where radioactive ground water exists, possibly sourced from potassic uranyl salts that formed from weathered phlogopite and scarce radioactive minerals in the kimberlite (Harris 1992). Much rarer examples of transparent green-coated diamonds recovered from alluvium are the Witwatersrand diamonds, where radioactivity in the groundwater probably originated from uraninite in the conglomerates.

In the alluvial environment a very low diamond concentration is matched by higher concentrations of radioactive minerals in the alluvium, which have been eroded from a wide range of surface crustal rocks over which a river system carrying diamonds has flowed. In this case radiation damage is the result of a particulate attack by α-particles from an adjacent radioactive mineral and the color intensity depends on the strength of the source and ranges in intensity from a pine green to a very dark green that almost appears black. The distribution of the radiation damage is controlled by the original distribution of the radioactive minerals in contact with the diamond (Fig. 47).

Brown radiation stains. If a green transparent coated or green stained diamond is heated in air to about 600 °C it very quickly turns irreversibly brown (Vance et al. 1973), perhaps indicating that brown naturally-irradiated diamonds have been heated to at least 600 °C post-eruption. Lawson et al. (1992) studied this transformation and showed that the reaction was kinetically controlled and heating experiments by Harris (unpublished) confirmed the time/temperature dependency. Attempts to use the kinetics of the reaction to determine the length of time to change green spots to brown spots has been thwarted because the error bar of the activation energy of the equation was relatively large. This resulted in a wide range of conversion periods for small adjustments of temperature (< 50 °C). For this reason, the equation was never used as a prospecting tool in diamond exploration.

The reason for the green-to-brown color change, is the temperature-driven local migration of vacancies (GR1) to one of two nitrogen aggregation sites (A and B centers), forming brown color centers known as H3 and H4 (Davies 1972; Mainwood 1994; Collins and Kiflawi 2009). The more this reaction proceeds, the darker the color. If the diamond with green stains is a Type II (containing virtually no nitrogen) then the second reaction does not occur. A detailed spectroscopic study of this color change is given by Nasdala et al. (2013). Figure 48 shows a typical array of brown radiation damage that can be associated on the same stone with green staining, signifying that radiation damage can occur at different stages in the life of an alluvial diamond.

Diamonds with green and brown radiation damage have been recovered from major placer deposits globally. Historically, irradiated diamonds were recovered from the Witwatersrand

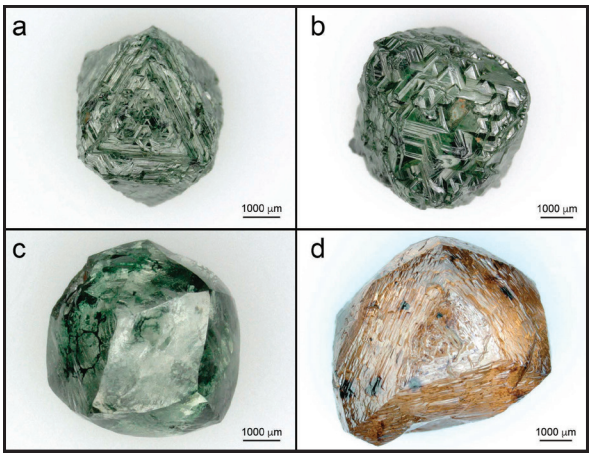

Figure 47. Alluvial diamonds from Guyana that have green and brown coloration from irradiation damage. [Images by Ellen Barrie (GIA).]

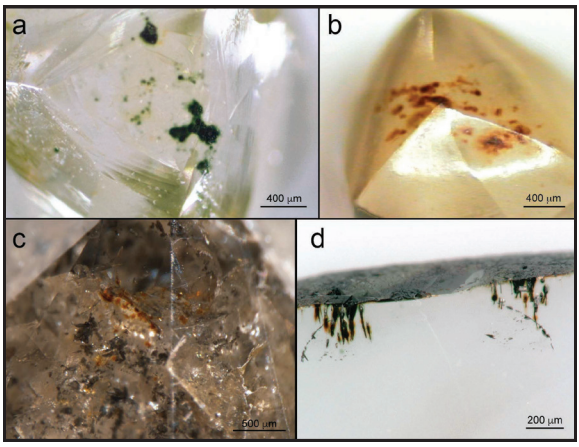

Figure 48. Alluvial diamonds with green and brown radiation stains (**a,b**) Diamonds from Namaqualand (South Africa) with staining on the surface. (**c,d**) Diamonds from Marange (Zimbabwe) with green and brown staining in fractures. [Images in (a,b) by Jeff Harris. Images in (c,d) by Karen Smit.]

basin in South Africa, where the presence of uranium-bearing minerals gave the diamonds significant color (Williams 1932; Gittus 1963; Raal and Robinson 1980). Such diamonds are now being recovered in the Diamantina district in Brazil (Karfunkel et al. 1995), the Quebrada Grande river basin in Venezuela (Kaminsky et al. 2000; Schulze et al. 2016) and most recently from the Marange deposit in Zimbabwe (Smit et al. 2018a).

An intriguing observation from color classification studies of diamonds from southern African mines (Harris et al. 1979) is that the high levels of transparent green coated diamonds recovered from the weathered upper portions of Finsch (South Africa) and Jwaneng (Botswana) (Harris et al. 1986) are not accompanied by a proportion of transparent brown diamonds. Eruption ages for Finsch and Jwaneng are 118 Ma and 240 Ma respectively (Gurney et al. 2005) and both diamond populations are not atypical. For the absence of a brown content the temperature in the primary environment had to be always below the temperature threshold for the second reaction to take place, or that radioactivity in the upper portion of the pipe must be a relatively recent event. The second possibility might explain the obvious presence of green and brown stains on

coastal alluvial diamonds from Namaqualand and Namibia to which the above mines may have contributed (see Kjarsgaard et al. 2022, this volume, and references therein). For Namibia, the diamond influx from the interior was Oligocene (~30 Ma) (Jacob and Grobbelaar 2019).

Concluding remarks

We have not described every surface feature known for diamond, but the above descriptions represent all the significant features and some of the rarer ones. Descriptions of surface features from specific countries have been completed on Russian diamonds (the Urals and Siberia) by Orlov (1977) and southern African diamonds by Robinson (1979). A classification scheme for surface features is outlined in Robinson et al. (1989). Tappert and Tappert (2011) provide excellent images and descriptions of the main surface features. The most recent and very detailed Canadian and Botswanan microdiamond study is by Fedortchouk (2019).

MINERAL INCLUSION MORPHOLOGY

Mineral impurities in diamond can be conveniently divided into those that are associated with diamond formation (*synchronous*) and those that occurred subsequently (*epigenetic*). *Synchronous* minerals are crystalline, invariably totally enclosed by the diamond and normally range in size from < 50 μm up to rare examples > 500 μm. *Epigenetic* minerals may form by the alteration of synchronous minerals and can occur in wholly internal fracture systems or in fractures with access to the exterior of the diamond.

Until recently, synchronous minerals were considered to have grown solely syngenetically with the diamond. This view has been challenged due to crystallographic (Nestola et al. 2014; Agrosi et al. 2016) and isotopic evidence (Westerlund et al. 2004; Smit et al. 2016a, 2019b; Aulbach et al. 2018). These studies have demonstrated that even if inclusions are protogenetic and crystallized before the host diamond, they can display textures indicative of co-crystallization (or syngenesis) (Figs. 49 and 50). Smit et al. (2022, this volume) shows that a lack of syngenecity is not necessarily a hindrance for inclusion-based diamond dating.

Synchronous inclusions

Synchronous inclusions consist principally of oxides, carbonates, silicates, and sulfides. Rare examples where diamond crystals are seen as distinct inclusions are found in Yakutian (Bulanova 1995) and Koffiefontein diamonds (Fig. 51a). Although graphite is more commonly observed as epigenetic inclusions (see below), rare synchronous graphite inclusions have been identified in diamond. At Ekati (Fig. 51b), the book-like layering and the characteristic shape of graphite inclusions may indicate that it has not had diamond morphology imposed on it. As conditions changed, the graphite preferentially expanded and caused the (111) fracture plane around the inclusion (Glinnemann et al. 2003). On a micron-scale synchronous graphite has also been identified as evenly distributed inclusions in cubo-octahedral diamonds from Marange, Zimbabwe (Fig. 21). In this case, their small size prevented identification of their shape, but their association with methane suggests that both phases crystallized from the diamond source fluid (Smit et al. 2016b).

The mineralogy and chemistry of synchronous mineral inclusions indicate that diamonds form through a wide range of depths in the deep Earth. The majority of diamonds form in the sub-continental lithospheric mantle (SCLM), and inclusions mainly represent both peridotitic and eclogitic host rocks, but with a minor websteritic environment defined by mineral chemistry rather than mineralogy alone (see review by Stachel and Harris 2008). Diamonds also form in the sub-lithospheric mantle (see review by Stachel et al. 2005). Mineral inclusion chemistry indicates their formation in the upper mantle (above 440 km), transition zone (between 440 and 660 km) and the lower mantle (below 660 km) (Harte et al. 1999; Kaminsky 2012; Pearson

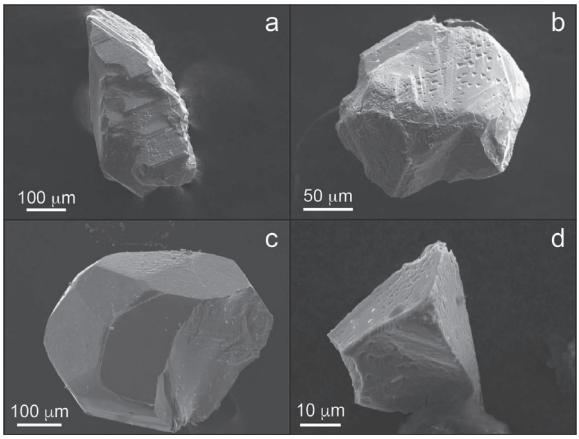

Figure 49. Secondary electron images showing cubo-octahedral morphologies in sulfide inclusions. These morphologies—including triangular step faces and trigons—are imposed by the diamond host, and are interpreted as evidence of co-crystallization of mineral inclusion and diamond host. (**a,b**) Eclogitic sulfides from Zimmi (Sierra Leone). (**c**) Eclogitic and (**d**) peridotitic sulfides from Ellendale (Australia). [Images by Karen Smit.]

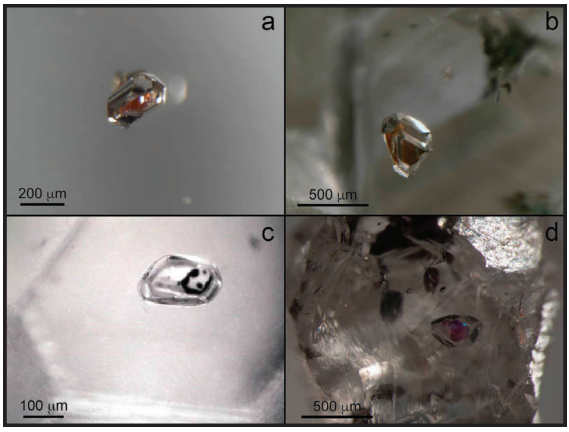

Figure 50. Cubo-octahedral morphologies in silicate inclusions. (**a,b**) Orange eclogitic garnet inclusions. (**c**) An elongate cubo-octahedral orthorhombic olivine inclusion in a matching cubo-octahedral Cullinan diamond (South Africa). (**d**) Purple-pink peridotitic garnet in a Koffiefontein diamond (South Africa). [Images in (a,b) by Karen Smit. Image in (c) by Jeff Harris. Image in (d) by Nicole Meyer (University of Alberta).]

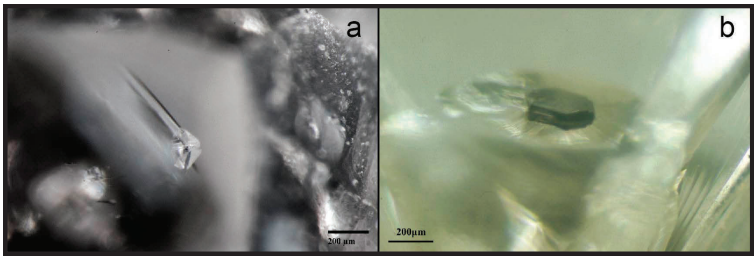

Figure 51. (**a**) Octahedral diamond crystal included in a diamond from Koffiefontein (South Africa). (**b**) Hexagonal graphite inclusion in an octahedral Ekati diamond (Canada). The graphite is stacked in 'book' form and is specifically oriented with respect to the diamond host. [Image in (a) by Nicole Meyer (University of Alberta). Image in (b) by Jeff Harris.]

et al. 2014; Burnham et al. 2016; Palot et al. 2017). The deepest diamonds that have been recovered formed in the lower mantle at depths of up to 800 km (Harte and Hudson 2013). Stachel et al. (2022, this volume) and Walter et al. (2022, this volume) give details on the mineral chemistry of lithospheric and sub-lithospheric inclusions.

Included minerals belong to all seven crystal systems and one might expect diverse inclusion morphology in diamond as a result. This is not the case, because all inclusion morphologies are influenced or imposed by the diamond host, leading to three shapes, common cubo-octahedra and rarer octahedra and cubes (Figs. 49, 50, 51, 52). Inclusions with cubo-octahedral, octahedral and cubic shapes may be equant or elongate, the latter invariably in diamond [110]. Morphologies may have recognizable faces over only part of the mineral, exhibit stepped surfaces parallel to those of the diamond, thicken or thin along particularly elongate inclusions (Fig. 52). Some inclusions may contain polymineralic intergrowths which can be clearly seen if the inclusion is elongate and there is a color distinction between two inclusions (Fig. 52d,f). More often such inclusions are identified after polishing for microprobe analyses. For examples of silicate and carbonate combinations see Phillips et al. (2004) and sulfide/garnet combinations are noted in Richardson et al. (2004) and Smit et al. (2019a). The crystallographic relationships between common peridotitic and eclogitic inclusions and their hosts are discussed in Angel et al. (2022, this volume).

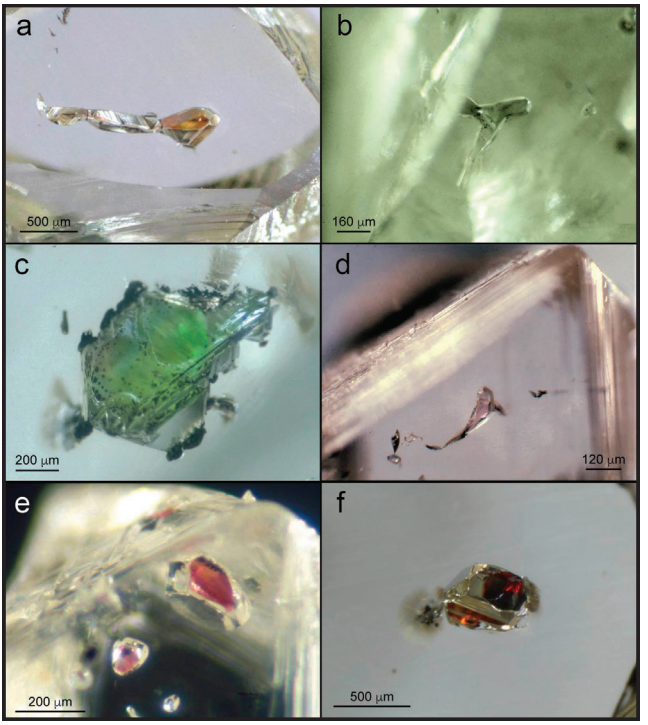

Figure 52. (**a**) Elongate orange garnet in diamond from the Urals (Russia), viewed through a (110) polished face. Well-defined cubo-octahedral faces give way to variable thickness and striations in reflectance along the length. (**b**) A bifurcation in a colorless inclusion in a Cullinan diamond (South Africa). (**c**) An elongate octahedral-shaped chrome diopside inclusion in a South African diamond. The dark material is graphite on the inclusion surface or in surrounding fractures. (**d**) A bi-mineralic peridotitic inclusion in a Cullinan diamond, comprising a purple garnet and a colourless mineral (either olivine or enstatite). (**e**) A flattish cubo-octahedral peridotitic garnet. (**f**) Bi-colored red and orange garnet inclusion—possibly eclogitic and pyroxenitic. For many inclusions, the color of the entire mineral is not visible due to the reflective interface between inclusion and diamond. [Images in (a–e) by Jeff Harris. Image in (f) by Karen Smit.]

Due to the reflective interface between mineral inclusion and diamond, inclusions can be partially obscured, and the color of the whole inclusion is not visible (Figs. 50 and 52). Along these interfaces between inclusions and diamonds, trapped fluids have recently been identified by Raman spectroscopy. In *lithospheric diamonds*, hydrous silicic fluid films of 1.5 μm maximum thickness were identified between diamond/inclusion interfaces (Nimis et al. 2016). All the principal peridotitic and eclogitic inclusions displayed fluid rims and the fluid composition was the same for both parageneses. A convenient explanation for the presence of this fluid is exsolution from the inclusions during eruptive decompression of the kimberlite or lamproite. Unfortunately, this is not the case, as chromite does not contain OH within its structure, yet still exhibited a fluid film. Thus the presence of these fluids reflects original incorporation of mantle fluids at the time of diamond growth (Nimis et al. 2016). In *sublithospheric diamonds*, fluid films comprised of reduced volatiles such as methane and hydrogen were found surrounding metallic inclusions in CLIPPIR diamonds and silicate inclusions in Type IIb diamonds (Fig. 53; Smith et al. 2016, 2018). In both these studies the fluid films were interpreted as a result of hydrogen escaping the inclusion and accumulating at the inclusion–host interface, with methane forming due to reaction of hydrogen with the surrounding carbon.

Metallic inclusions in newly-recognized CLIPPIR diamonds frequently occur along a <111> direction, as chains of inclusions that developed during brittle-plastic deformation in the mantle (Fig. 54; Smith et al. 2017).

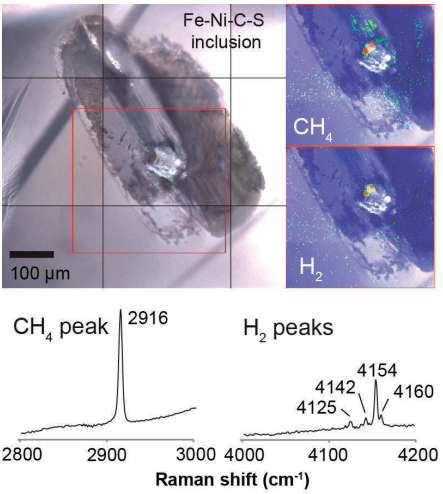

Figure 53. Minerals trapped in sub-lithospheric diamond may also develop internal fractures as a result of the extremely high residual pressure. Reduced fluid films around some sub-lithospheric inclusions have been identified by Raman spectroscopy. [Reproduced from Smith et al. (2016b) Large gem diamonds from metallic liquid in Earth's deep mantle. Science 354:1403–1405. Used with permission from the American Academy for the Advancement of Science.]

Epigenetic inclusions

Internal fractures in diamond arise either as a release of general stress within the stone or occur specifically around some synchronous inclusions, where differential thermal expansion is the cause (Figs. 53–55). Invariably in both cases fractures occur along diamond's {111} cleavage planes. Both of these occurrences often contain secondary dull black graphite of variable micron size. Stress release graphite takes the form of single or multiple disc-like clusters, probably occurring as a consequence of fracture formation, the {111} surfaces being the easiest way graphite can form from diamond (Fig. 56a). When analyzed by Raman spectroscopy, epigenetic graphite often shows highly amorphous/disordered structures (Khokhryakov and Nechaev 2015).

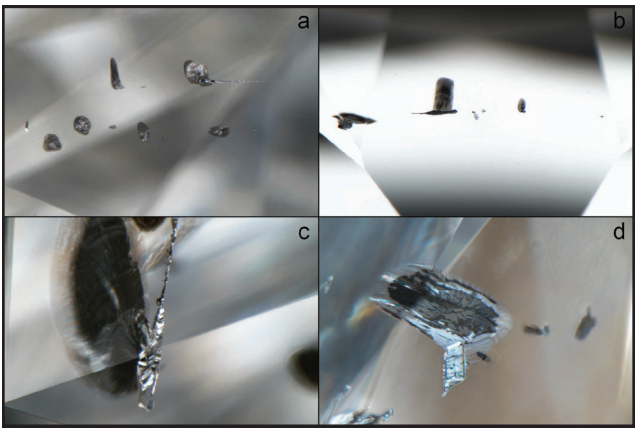

Figure 54. Examples of the typical appearance of metallic Fe-Ni-C-S inclusions in CLIPPIR diamonds. (**a**) Two parallel <111> oriented chains (field of view 2.34 mm). (**b**) Backlit inclusion chain (field of view 1.42 mm). (**c**) Elongate metallic inclusion with a round black fracture of {111} orientation that obliquely cuts the <111> elongation direction of the inclusion (field of view 1.42 mm). (**d**) A less elongate metallic inclusion with a small irregular tail on the lower left (field of view 1.42 mm). [Reproduced from Smith et al. (2017), Gems and Gemology. Used with permission.]

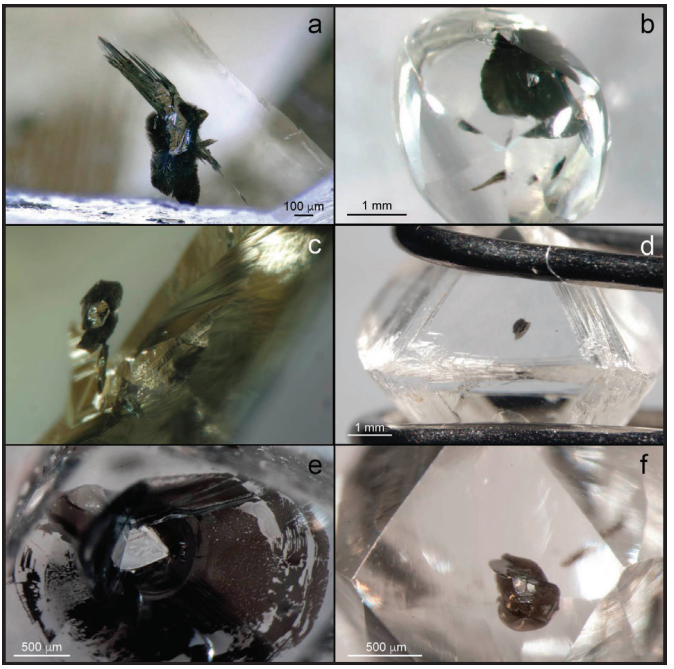

Figure 55. Fractures around sulfide inclusions, arising as a result of differential stress release during kimberlite eruption. Fractures typically develop along diamond's {111} cleavage planes. Size of the fractures is not always proportional to the size of the sulfide. [Images in (a-d) by Karen Smit. Images in (e-f) by Nicole Meyer (University of Alberta).]

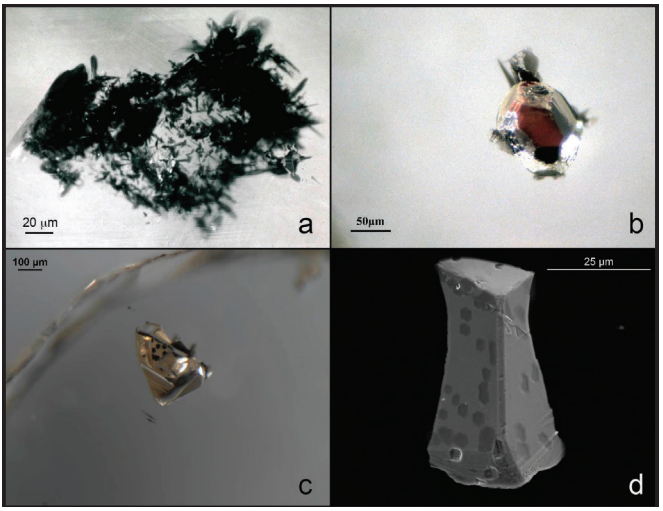

Figure 56. (**a**) A cluster of graphite flakes lying in the four equivalent cleavage planes of a South African diamond. (**b**) A peridotitic garnet inclusion in a diamond from Ghana showing graphite development principally at the inclusion coigns. (**c**) Hexagonal graphite flakes on an orange eclogitic garnet still encapsulated in a diamond. (**d**) Hexagonal graphite flakes on a sulfide inclusion broken out of a diamond. [Images in (a,b) by Jeff Harris. Images in (c,d) by Karen Smit.]

Where visible inclusions are involved, graphite may have an uneven distribution around the mineral itself with noticeable concentrations at inclusion coigns (Fig. 56b). Also if an inclusion face is parallel to an octahedral diamond plane some interfaces are decorated with graphite in the form of irregular flakes, or with hexagonal outlines (Fig. 56c–d).

Vacuum experiments by Harris and Vance (1972) created graphite around inclusions at temperature as low as 900 °C, the authors believing that the graphite reaction was caused by the release of carbon dioxide from the inclusion. With the later discovery of fluid films (Nimis et al. 2016; Smith et al. 2016b, 2018), a more adequate explanation is a reaction between diamond and the fluid. Graphite flakes on inclusion/diamond interfaces may relate to uneven distribution of the fluid film leading to only isolated reactions (Fig. 56b–d).

Sulfides have the greatest differential thermal expansion of all the inclusions and their internal fracture systems are relatively large and have a rosette appearance. The dark material in these fractures has a distinct metallic luster, which distinguishes it from graphite (Fig. 55). The fracture infilling is a consequence of a quantity of sulfide being extruded into the fractures from the central inclusion. This likely occurred at the time of fracturing and is due to sulfide plasticity at high temperatures.

Materials in external fractures have their origins either whilst diamond is still in the rocks that brought them to Earth's surface or within an alluvial environment once weathered out of those rocks. With alluvial diamonds, the more vigorous nature of that environment especially during transport certainly causes some diamonds to fracture and might allow ingress of secondary material. Because pseudomorphs are usually found with typical inclusion outlines (Fig. 57) their formation is most likely linked to an alteration of the inclusion through a surface-connected fracture, probably still in a kimberlitic/lamproitic environment where high temperature and volatiles aid the transformation.

Figure 57. Two inclusions with the typical features of varying shape, as well as graphite on inclusion interfaces and in stress fractures. However, after X-ray analyses, both crystals were identified as powdered goethite, probably pseudomorphs after olivine or enstatite. Inclusions are in a diamond from Ghana. [Image by Jeff Harris.]

FINAL REMARKS

Much credit for our understanding of the morphology and surface features of diamond should go to those early notables, such as Fersmann and Goldschmidt (1911), Sutton (1928) and Williams (1932) who gathered together diamonds and laboriously drew beautifully detailed shape and surface feature characteristics of representative examples. Several early authors noted the presence of rounded surfaces on many diamonds, though it wasn't until the 1970s that it was accepted that these rounded surfaces were not growth features, but rather the result of dissolution (Moore and Lang 1972).

More recent works on diamond morphology have focused on understanding the formation conditions for the wide variety of surface features (e.g., Robinson 1979; Robinson et al. 1986). Experimental work covering a range of pressures, temperatures and fluid compositions has shown the specific formation conditions for features expected to form either in the diamond stability field, or during kimberlite and lamproite eruption (Khokhryakov and Pal'yanov 2007, 2010; Fedortchouk et al. 2019).

The literature on diamond morphology, internal growth, surface features and the shapes of inclusions is extensive. Tappert and Tappert (2011) have provided an excellent starting point, with an overview of the main morphological features of natural diamonds accompanied by superlative images. For those wishing to further consider the morphology of diamond and its mineral inclusions, the Proceedings Volumes and Extended Abstracts of the 11 International Kimberlite Conferences (1973–2018) will be very useful. The *Journal of the International Kimberlite Conferences* can be found at *https://journals.library.ualberta.ca/ikcabstracts.com*.

DIRECTIONS FOR FUTURE WORK

External and Internal Morphology. One area which might still be explored is the relationship between micro- and macro-diamonds to clarify whether the micros are simply smaller equivalents of the macro-populations, or whether they represent separate distinct growth events. This distinction may seem trivial but it has important implications during the economic evaluation of a kimberlite, and whether the characteristics of microdiamond populations can be extrapolated to larger sizes. This type of study likely requires a combined approach using CL to investigate internal growth features, inclusion studies, and geochemical studies of the diamond (carbon isotopes, nitrogen isotopes, trace elements).

We have shown the complexity of the internal growth of some diamonds. There are still many internal growth features that cannot be explained, and will only be resolved with further work. Up to now experimental work has largely concentrated on how an already formed diamond can change shape with respect to varying conditions. Perhaps further experiments can investigate how CL patterns develop in synthetic diamonds grown under a range of growth rates, pressure and temperature conditions and in different geological fluids.

Surface features. In almost any diamond parcel there are diamond crystals with unusual surface features, whose origins are still difficult to interpret. In the last decades, experimental studies were able to produce many dissolution features present on natural diamonds and to determine the controlling factors for their development. Some diamond surface features show a strong association with the host kimberlite lithology and with the behavior of volatiles during kimberlite ascent and emplacement. Using the information stored in the surface dissolution features of diamonds, further studies may help to constrain the formation of the different types of kimberlites and the mechanism of magma emplacement. Integrating studies of cathodoluminescence growth patterns of diamonds with dissolution surface features produced during mantle residence, should help to better understand the nature of diamond-growth and diamond-destructive metasomatic events in the sub-cratonic mantle. The study of fluids resulting in surface features on a wide variety of different diamonds may provide a broader understanding of carbon fluids in the deep Earth.

Inclusions. One of the main outstanding issues around mineral inclusion morphology is whether an inclusion was pre-existing in the lithosphere prior to diamond formation or whether it crystallized when the diamond source fluid was introduced into the lithosphere. Regardless, inclusions always have cubo-octahedral morphologies because they co-crystallize with the diamond. Though this may sound trivial, the distinction has implications for geothermobarometry (which depends on major and trace element equilibrium between different mineral inclusions) and geochronology (whether there was isotopic equilibrium between minerals). These issues are being addressed with the help of crystallographic work on mineral inclusions and their host diamonds (Angel et al. 2022, this volume). The implications for geothermobarometry and geochronology are discussed in Nimis (2022, this volume) and Smit et al. (2022, this volume).

Minerals found trapped in diamonds are the only pristine samples we have of the deep Earth, and there is considerable research emphasis on using these valuable mineral inclusions to understand mantle processes in the lithosphere and sub-lithospheric regions like the upper mantle, transition zone and lower mantle. Although the inclusion population in diamond is considerable and diverse, new minerals are continually discovered. All one needs is a supply of diamonds, a (Raman) microscope and a great deal of patience.

ACKNOWLEDGEMENTS

We thank Ingrid Chinn, Tom McCandless and the editor Graham Pearson, for their constructive reviews that improved the quality of our manuscript. Thank you to Wuyi Wang and Tom Moses for their permission to use unpublished GIA images.

REFERENCES

Agrosi G, Nestola F, Tempesta G, Bruno M, Scandale E, Harris J (2016) X-ray topographic study of a diamond from Udachnaya; implications for the genetic nature of inclusions. Lithos 248–251:153–159

Akagi T, Masuda A (1988) Isotopic and elemental evidence for a relationship between kimberlite and Zaire cubic diamonds. Nature 336:665–667

Angel RJ, Alvaro M, Nestola F (2022) Crystallographic methods for non-destructive characterization of mineral inclusions in diamonds. Rev Mineral Geochem 88:257–306
Arima M, Kozai Y (2008) Diamond dissolution rates in kimberlitic melts at 1300–1500 °C in the graphite stability field. Eur J Mineral 20:357–364
Aulbach S, Stachel T, Creaser RA, Heaman LM, Shirey SB, Muehlenbachs K, Eichenberg D, Harris JW (2009) Sulphide survival and diamond genesis during formation and evolution of Archaean subcontinental lithosphere; a comparison between the Slave and Kaapvaal Cratons. Lithos 112:747–757
Aulbach S, Creaser RA, Stachel T, Heaman LM, Chinn IL, Kong J (2018) Diamond ages from Victor (Superior Craton); intra-mantle cycling of volatiles (C, N, S) during supercontinent reorganisation. Earth Planet Sci Lett 490:77–87
Bovenkerk HP (1961) Some observations on the morphology and physical characteristics of synthetic diamond. Am Mineral 46:952–963
Boyd SR, Mattey DP, Pillinger CT, Milledge HJ, Mendelssohn M, Seal M (1987) Multiple growth events during diamond genesis; an integrated study of carbon and nitrogen isotopes and nitrogen aggregation state in coated stones. Earth Planet Sci Lett 86:341–353
Bragg WH, Bragg WL (1913) The structure of the diamond. Nature 91:557–557
Bragg WH, Bragg WL (1914) The structure of the diamond. Proc R Soc London A 89:277–291
Bulanova GP (1995) The formation of diamond. *In:* Diamond Exploration into the 21st Century. Vol 53; 1–3. Griffin WL, (ed) Elsevier, Amsterdam-New York, International, p 1–23
Bulanova GP, Griffin WL, Kaminsky FV, Davies RM, Spetsius ZV, Ryan CG, Andrew AS, Zahkarchenko OD (1999) Diamonds from Zarnitsa and Dalnaya kimberlites (Yakutia), their nature and lithospheric mantle source. *In:* Proceedings of the VIIth international kimberlite conference; Vol 1. Gurney JJ, Gurney JL, Pascoe MD, Richardson SH, (eds). Red Roof Design, Cape Town, South Africa, p 49–56
Bulanova GP, Pearson DG, Hauri EH, Griffin BJ (2002) Carbon and nitrogen isotope systematics within a sector-growth diamond from the Mir Kimberlite, Yakutia. Chem Geol 188:105–123
Bulanova GP, Wiggers de Vries DF, Pearson DG, Beard A, Mikhail S, Smelov AP, Davies GR (2014) An eclogitic diamond from Mir Pipe (Yakutia), recording two growth events from different isotopic sources. Chem Geol 381:40–54
Burnham AD, Bulanova GP, Smith CB, Whitehead SC, Kohn SC, Gobbo L, Walter MJ, Shirey SB (2016) Diamonds from the Machado River alluvial deposit, Rondonia, Brazil, derived from both lithospheric and sublithospheric mantle. Lithos 265:199–213
Chepurov AI, Khokhryakov AF, Sonin VM, Pal yYN (1985) Forms of dissolution of diamond crystals in high-temperature silicate solutions. Doklady Akademii Nauk SSSR 285:212–216 (in Russian)
Clement CR, Harris JW, Robinson DN, Hawthorne JB (1986) The De Beers kimberlite pipe; a historic South African diamond mine. *In:* Mineral deposits of Southern Africa. Anhaeusser CR, Maske S (eds). Geol Soc S Afr, Johannesburg, South Africa, p 2193–2214
Collins AT (1982) A spectroscopic survey of naturally-occurring vacancy-related colour centres in diamond. J Phys D: App Phys 15:1431–1438
Collins AT, Kiflawi I (2009) The annealing of radiation damage in type Ia diamond. J Phys Condens Matter 21:364209
Collins AT, Kanda H, Kitawaki H (2000) Colour changes produced in natural brown diamonds by high-pressure, high-temperature treatment. Diam Relat Mater 9:113–122
Davies G (1972) The effect of nitrogen impurity on the annealing of radiation damage in diamond. J Physics C: Solid State Phys 5:2534–2542
Davies RM, Griffin WL, O'Reilly SY, Doyle BJ, Mitchell RH, Gruetter HS, Heaman LM, Scott Smith BH, Stachel T (2004) Mineral inclusions and geochemical characteristics of microdiamonds from the DO27, A154, A21, A418, DO18, DD17 and Ranch Lake kimberlites at Lac de Gras, Slave Craton, Canada. Lithos 77:39–55
DeVries RC (1975) Plastic deformation and "work-hardening" of diamond. Mater Res Bull 10:1193–1199
Evans T, Sauter DH (1961) Etching of diamond surfaces with gases. Philos Mag 6:429–440
Evans T, Wild RK (1965) Plastic bending of diamond plates. Philos Mag 12:479–489
Fedortchouk Y (2015) Diamond resorption features as a new method for examining conditions of kimberlite emplacement. Contrib Mineral Petrol 170:36
Fedortchouk Y (2019) A new approach to understanding diamond surface features based on a review of experimental and natural diamond studies. Earth Sci Rev 193:45–65
Fedortchouk Y, Zhang Z (2011) Diamond resorption; link to metasomatic events in the mantle or record of magmatic fluid in kimberlitic magma? Can Mineral 49:707–719
Fedortchouk Y, Canil D, Semenets E (2007) Mechanisms of diamond oxidation and their bearing on the fluid composition in kimberlite magmas. Am Mineral 92:1200–1212
Fedortchouk Y, Canil D, Comodi P, Nestola F, Angel RJ (2009) Diamond oxidation at atmospheric pressure; development of surface features and the effect of oxygen fugacity. Eur J Mineral 21:623–635
Fedortchouk Y, Matveev S, Carlson JA (2010) H_2O and CO_2 in kimberlitic fluid as recorded by diamonds and olivines in several Ekati diamond mine kimberlites, Northwest Territories, Canada. Earth Planet Sci Lett 289:549–559
Fedortchouk Y, Chinn IL, Kopylova MG (2017) Three styles of diamond resorption in a single kimberlite; effects of volcanic degassing and assimilation. Geology (Boulder) 45:871–874

Fedortchouk Y, Liebske C, McCammon C (2019) Diamond destruction and growth during mantle metasomatism; an experimental study of diamond resorption features. Earth Planet Sci Lett 506:493–506
Fersman AE (1955) Crystallography of Diamond (Classics of Science). USSR Acad Sci, Moscow (in Russian)
Fersmann A, Goldschmidt V (1911) Der Diamant: Eine Studie. Carl Winter's Universitatbuchhandlung, Heidelberg
Fisher D, Sibley S, Kelly C (2009) Brown colour in natural diamond and interaction between the brown related and other colour-inducing defects. J Phys Condens Matter 21:364213
Frank FC, Lang AR (1965) X-ray topography of diamond. *In*: Physical Properties of Diamond. Berman R, (ed) Clarendon Press, Oxford, England, p 69–115; especially 86–102
Frank FC, Puttick KE, Wilks EM (1958) Etch pits and trigons on diamond: I. Philos Mag 3:1262–1272
Gaillou E, Post J, Bassim N, Zaitsev A, Rose T, Fries M, Stroud R, Steele A, Butler J (2010) Spectroscopic and microscopic characterizations of color lamellae in natural pink diamonds. Diam Relat Mater 19:1207–1220
Gaillou E, Post JE, Rose T, Butler JE (2012) Cathodoluminescence of natural, plastically deformed pink diamonds. Micros Microanal 18:1–11
Gittus JH (1963) Uranium. Metallurgy of the Rare Metals Vol 8. Butterworths, London
Glinnemann J, Kusaka K, Harris JW (2003) Oriented graphite single-crystal inclusions in diamond. Z Kristallog Cryst Mater 218:733–739
Graham RJ, Moustakas TD, Disko MM (1991) Cathodoluminescence imaging of defects and impurities in diamond films grown by chemical vapor deposition. J Appl Phys 69:3212–3218
Grantham DR, Allen JB (1960) Kimberlite in Sierra Leone. *In:* Overseas Geology and Mineral Resources. Quarterly Bulletin of the Overseas Geological Surveys. EH Beard (ed) Vol. 8, p 5–25
Green BL, Collins AT, Breeding CM (2022) Diamond spectroscopy, defect centers, color, and treatments. Rev Mineral Geochem 88:637–688
Gurney JJ, Hildebrand PR, Carlson JA, Fedortchouk Y, Dyck DR (2004) The morphological characteristics of diamonds from the Ekati property, Northwest Territories, Canada. Lithos 77:21–38
Gurney JJ, Helmstaedt HH, Le Roex AP, Nowicki TE, Richardson SH, Westerlund KJ, Hedenquist JW, Thompson JFH, Goldfarb RJ, Richards JP (2005) Diamonds; crustal distribution and formation processes in time and space and an integrated deposit model. Econ Geol 100:143–177
Hall AE, Smith CB (1984) Lamproite diamonds; are they different? *In:* Kimberlite occurrence and origin; a basis for conceptual models in exploration. Vol 8. Glover JE, Harris PG, (eds). University of Western Australia, Geology Department and Extension Service. Perth, Australia, p 167–212
Hanley PL, Kiflawi I, Lang AR (1977) On topographically identifiable sources of cathodoluminescence in natural diamonds. Phil Trans R Soc London Ser A 284:329–368
Harlow GE (1998) The Nature of Diamonds. Cambridge University Press, Cambridge, United Kingdom
Harris JW (1992) Diamond geology. *In:* The Properties of Natural and Synthetic Diamond. Field JE (ed) Academic Press, London, p 345–394
Harris JW, Vance ER (1972) Induced graphitisation around crystalline inclusions in diamond. Contrib Mineral Petrol 35:227–234
Harris JW, Hawthorne JB, Oosterveld M, Wehmeyer E (1975) A classification scheme for diamond and a comparative study of South African diamond characteristics. Phys Chem of the Earth 9:765–783
Harris JW, Hawthorne JB, Oosterveld MM (1979) Regional and local variations in the characteristics of diamonds from some southern African kimberlites. *In:* Kimberlites, diatremes, and diamonds; their geology, petrology, and geochemistry. Vol 1. Boyd FR, Meyer HOA, (eds). Am Geophys Union, Washington, United States, p 27–41
Harris JW, Hawthorne JB, Oosterveld MM (1983) A comparison of diamond characteristics from the De Beers Pool mines, Kimberley, South Africa. *In:* Kimberlites III; Documents. Vol 74. Kornprobst J, (ed) Ann Sci Univ Clermont II, Clermont-Ferrand, France, p 1–13
Harris JW, Hawthorne JB, Oosterveld MM (1986) A comparison of characteristics of diamonds from the Orapa and Jwaneng kimberlite pipes in Botswana. *In:* Vol 16 Extended Abstracts, IVth International Kimberlite Conference. Smith CB, (ed) Geol Soc Australia, Sydney, Australia, p 395–397
Harrison ER, Tolansky S (1964) Growth history of a natural octahedral diamond. Proc R Soc London A 279:490–496
Harte B, Hudson N (2013) Mineral associations in diamonds from the lowermost upper mantle and uppermost lower mantle. Proc 10th Int Kimberlite Confer, p. 235–253
Harte B, Harris JW, Hutchison MT, Watt GR, Wilding MC (1999) Lower mantle mineral associations in diamonds from Sao Luiz, Brazil. *In:* Mantle petrology; field observations and high-pressure experimentation; a tribute to Francis R (Joe) Boyd. Vol 6. Fei Y, Bertka Constance M, Mysen Bjorn O, (eds). Geochemical Society - University of Houston, Department of Chemistry, Houston, TX, United States, p 125–153
Howell D, Griffin WL, Piazolo S, Say JM, Stern RA, Stachel T, Nasdala L, Rabeau JR, Pearson NJ, O'Reilly SY (2013) A spectroscopic and carbon-isotope study of mixed-habit diamonds; impurity characteristics and growth environment. Am Mineral 98:66–77
Howell D, Stern RA, Griffin WL, Southworth R, Mikhail S, Stachel T (2015) Nitrogen isotope systematics and origins of mixed habit diamonds. Geochim Cosmochim Acta 157:1–12

Jacob J, Grobbelaar G (2019) Onshore and nearshore diamond mining on the south-western coast of Namibia: Recent activities and future exploration techniques. J Gemm 36:524–532
Jacob DE, Mikhail S (2022) Polycrystalline diamonds from kimberlites: Snapshots of rapid and episodic diamond formation in the lithospheric mantle. Rev Mineral Geochem 88:167–190
Kaminsky F (2012) Mineralogy of the lower mantle; a review of "super deep" mineral inclusions in diamond. Earth-Sci Rev 110:127–147
Kaminsky FV, Khachatryan GK (2004) The relationship between the distribution of nitrogen impurity centres in diamond crystals and their internal structure and mechanism of growth. Lithos 77:255–271
Kaminsky FV, Zakharchenko OD, Griffin WL, Channer DMD, Khachatryan BGK (2000) Diamond from the Guaniamo area, Venezuela. Can Mineral 38:1347–1370
Kamiya Y, Lang AR (1965) On the structure of coated diamonds. Philos Mag 11:347–356
Karfunkel J, Chaves MLSC, Svisero DP, Meyer HOA (1995) Diamonds from Minas Gerais, Brazil; an update on sources, origin, and production. Int Geol Rev 36:1019–1032
Khokhryakov AF, Nechaev DV (2015) Typomorphic features of graphite inclusions in diamond: experimental data. Russ Geol Geophys 56:232–238
Khokhryakov AF, Pal'yanov YN (2007) The evolution of diamond morphology in the process of dissolution; experimental data. Am Mineral 92:909–917
Khokhryakov AF, Pal'yanov YN (2009) Origin of drop-shaped hillocks on tetrahexahedroids of natural diamonds. Proceedings of the Annual Session of Russian Mineralogical Society "Ontogeny of minerals applied to scientific and industrial uses (to the 100 year anniversary of Prof. Dmitry Grigoriev)", St. Petersburg, 153–155 (in Russian)
Khokhryakov AF, Pal'yanov YN (2010) Influence of the fluid composition on diamond dissolution forms in carbonate melts. Am Mineral 95:1508–1514
Kiflawi I, Collins A, Lakoubovskii K, Fisher D (2007) Electron irradiation and the formation of vacancy–interstitial pairs in diamond. J Phys Condens Matter 19:046216
Kjarsgaard BA, de Wit M, Heaman LM, Pearson DG, Stiefenhofer J, Janusczcak N, Shirey SB (2022) A review of the geology of global diamond mines and deposits. Rev Mineral Geochem 88:1–118
Kozai Y, Arima M (2005) Experimental study on diamond dissolution in kimberlitic and lamproitic melts at 1300–1420 °C and 1 GPa with controlled oxygen partial pressure. Am Mineral 90:1759–1766
Lang AR (1964) Dislocations in diamond and the origin of trigons. Proc R Soc London A 278:234–242
Lang AR (1974a) On the growth-sectorial dependence of defects in natural diamonds. Proc R Soc London A 340:233–248
Lang AR (1974b) Glimpses into the growth history of natural diamonds. J Cryst Growth 24/25:108–115
Lang AR (1979) Internal structure. *In:* The properties of diamond. Field JE, (ed) Acad. Press, London, United Kingdom, p 425–469
Lang AR, Bulanova GP, Fisher D, Furkert S, Sarua A (2007) Defects in a mixed-habit Yakutian diamond: Studies by optical and cathodoluminescence microscopy, infrared absorption, Raman scattering and photoluminescence spectroscopy. J Cryst Growth 309:170–180
Lawson S, Davies G, Collins AT, Mainwood A (1992). Migration energy of the neutral vacancy in diamond. J Phys Condens Matter 4:L125–L131
Li ZY, Fedortchouk Y, Fulop A, Chinn IL, Forbes N (2018) Positively oriented trigons on diamonds from the Snap Lake kimberlite dike, Canada: Implications for fluids and kimberlite cooling rates. Am Mineral 103:1634–1648
Lu T, Shigley J, Koivula J, Reinitz I (2001) Observation of etch channels in several natural diamonds. Diam Relat Mater 10:68–75
Lüttge A (2006) Crystal dissolution kinetics and Gibbs free energy. J Electron Spectrosc 150:248–259
Machado WG, Moore M, Woods GS (1985) On the dodecahedral growth of coated diamonds. J Cryst Growth 71:718–727
Machado WG, Moore M, Yacoot A (1998) Twinning in natural diamond. II. interpenetrant cubes. J Appl Crystallogr 31:777–782
Mainwood A (1994) Nitrogen and nitrogen-vacancy complexes and their formation in diamond. Phys Rev B 49:7934–7940
Mineeva R, Speransky A, Titkov S, Zudin N (2007) The ordered creation of paramagnetic defects at plastic deformation of natural diamonds. Phys Chem Minerals 34:53–58
Mitchell RH (1986) Kimberlites: Mineralogy, Geochemistry, and Petrology. Plenum Press, New York
Moore M (1985) Diamond morphology. Industrial Diamond Rev 45:67–71
Moore M (2009) Imaging diamond with X-rays. J Phys Condens Matter 21:364217
Moore M, Lang AR (1972) On the internal structure of natural diamonds of cubic habit. Philos Mag 26:1313–1325
Moore M, Lang AR (1974) On the origin of the rounded dodecahedral habit of natural diamond. J Cryst Growth 26:133–139
Moses TM, Shigley JE, McClure S, Koivula J, Daele M (1999) Observations on GE-processed diamonds: A photographic record. Gem Gemol 35:14–22
Nailer SG, Moore M, Chapman J, Kowalski G (2007) On the role of nitrogen in stiffening the diamond structure. J Appl Crystallogr 40:1146–1152
Nasdala L, Grambole D, Wildner M, Gigler AM, Hainschwang T, Zaitsev AM, Harris JW, Milledge J, Schulze DJ, Hofmeister W, Balmer WA(2013) Radio colouration of diamond; a spectroscopic study. Contrib Mineral Petrol 165:843–861

Navon O, Hutcheon ID, Rossman GR, Wasserburg GJ (1988) Mantle-derived fluids in diamond micro-inclusions. Nature (London) 335:784–789
Nestola F, Nimis P, Angel RJ, Milani S, Bruno M, Prencipe M, Harris JW (2014) Olivine with diamond-imposed morphology included in diamonds; syngenesis or protogenesis? Int Geol Rev 56:1658–1667
Nimis P (2022) Pressure and temperature data for diamonds. Rev Mineral Geochem 88:533–566
Nimis P, Alvaro M, Nestola F, Angel RJ, Marquardt K, Rustioni G, Harris JW, Marone F (2016) First evidence of hydrous silicic fluid films around solid inclusions in gem quality diamonds. Lithos 260:384–389
Orlov YL (1977) The mineralogy of the diamond. John Wiley and Sons, New York N.Y., United States
Palot M, Pearson DG, Stachel T, Stern RA, Le Pioufle A, Gurney JJ, Harris JW (2017) The transition zone as a host for recycled volatiles: Evidence from nitrogen and carbon isotopes in ultra-deep diamonds from Monastery and Jagersfontein (South Africa). Chem Geol 466:733–749
Pandeya D, Tolansky S (1961) Micro-disk patterns on diamond dodecahedra. Proc Phys Soc 78:12–16
Pearson DG, Brenker FE, Nestola F, McNeill J, Nasdala L, Hutchison MT, Matveev S, Mather K, Silversmit G, Schmitz S, Vekemans B (2014) Hydrous mantle transition zone indicated by ringwoodite included within diamond. Nature 507:221–224
Petts DC, Stachel T, Stern RA, Hunt L, Fomradas G (2016) Multiple carbon and nitrogen sources associated with the parental mantle fluids of fibrous diamonds from Diavik, Canada, revealed by SIMS microanalysis. Contrib Mineral Petrol 171:17
Phillips D, Harris JW, Viljoen KS (2004) Mineral chemistry and thermobarometry of inclusions from De Beers Pool diamonds, Kimberley, South Africa. Lithos 77:155–179
Raal FA, Robinson DN (1980) Green for rarity. Nuclear Active 23:5–8
Rakovan J, Gaillou E, Post JE, Jaszczak JA, Betts JH (2014) Optically sector-zoned (star) diamonds from Zimbabwe, Rocks & Minerals 89:2:173–178
Richardson SH, Shirey SB, Harris JW (2004) Episodic diamond genesis at Jwaneng, Botswana, and implications for Kaapvaal Craton evolution. Lithos 77:143–154
Robinson DN (1979) Surface textures and other features of diamonds. PhD Dissertation, University of Cape Town
Robinson DN, Scott JA, Van NA, Anderson VG (1986) Events reflected in the diamonds of some Southern African kimberlites. *In:* Vol 16 Extended Abstracts, IVth International Kimberlite Conference. Smith CB, (ed) Geological Society of Australia, Sydney, Australia: 421–423
Robinson DN, Scott JA, Van NA, Anderson VG (1989) The sequence of events reflected in the diamonds of some Southern African kimberlites. *In:* Kimberlites and related rocks. Vol 14; 2. Ross J, Jaques AL, Ferguson J, Green DH, Y ORS, Danchin RV, Janse AJA (eds) Geological Society of Australia, Sydney, Australia, p 990–1000
Rondeau B, Fritsch E, Moore M, Thomassot E, Sirakian JF (2007) On the growth of natural octahedral diamond upon a fibrous core. J Cryst Growth 304:287–293
Schulze DJ, Nasdala L, Shirey SB (2016) Unusual paired pattern of radiohaloes on a diamond crystal from Guaniamo (Venezuela). Lithos 265:177–181
Seager AF (1979) The origin of a tetrahedral diamond. Mineral Mag 43:377–387
Seal M (1965) Structure in diamonds as revealed by etching. Am Mineral 50:105–123
Shirey SB, Richardson SH (2011) Start of the Wilson cycle at 3 Ga shown by diamonds from subcontinental mantle. Science 333:434–436
Shor R, Weldon R, Janse AJA, Breeding C, Shirey S (2015) Letšeng's unique diamond proposition. Gem Gemol 51:280–299
Smit KV, Shirey SB, Wang W (2016a) Type Ib diamond formation and preservation in the West African lithospheric mantle; Re/Os age constraints from sulphide inclusions in Zimmi diamonds. Precambrian Res 286:152–166
Smit KV, Shirey SB, Stern RA, Steele A, Wang W, Shirey SB (2016b) Diamond growth from C–H–N–O recycled fluids in the lithosphere; evidence from CH_4 micro-inclusions and $\delta^{13}C$–$\delta^{15}N$–N content in Marange mixed-habit diamonds. Lithos 265:68–81
Smit KV, Myagkaya E, Persaud S, Wang W (2018a) Black diamonds from Marange (Zimbabwe): a result of natural irradiation and graphite inclusions. Gem Gemol 11:177
Smit KV, D'Haenens-Johansson UFS, Howell D, Loudin LC, Wang W (2018b) Deformation-related spectroscopic features in natural Type Ib-IaA diamonds from Zimmi (West African craton). Miner Petrol 112:243–257
Smit KV, Stachel T, Luth RW, Stern RA (2019a) Evaluating mechanisms for eclogitic diamond growth; an example from Zimmi Neoproterozoic diamonds (West African Craton). Chem Geol 520:21–32
Smit KV, Shirey SB, Hauri EH, Stern RA (2019b) Sulfur isotopes in diamonds reveal differences in continent construction. Science 364:383
Smit KV, Timmerman S, Aulbach S, Shirey SB, Richardson SH, Phillips D, Pearson DG (2022) Geochronology of diamonds. Rev Mineral Geochem 88:567–636
Smith CB, Walter MJ, Bulanova GP, Mikhail S, Burnham AD, Gobbo L, Kohn C (2016a) Diamonds from Dachine, French Guiana: A unique record of early Proterozoic subduction. Lithos 265:82–95
Smith EM, Shirey SB, Nestola F, Bullock ES, Wang J, Richardson SH, Wang W (2016b) Large gem diamonds from metallic liquid in Earth's deep mantle. Science 354:1403–1405
Smith EM, Shirey SB, Wang W (2017) The very deep origin of the world's biggest diamonds. Gem Gemol 53:388–403

Smith EM, Shirey SB, Richardson SH, Nestola F, Bullock ES, Wang J, Wang W (2018) Blue boron-bearing diamonds from Earth's lower mantle. Nature 560:84–87
Spetsius Z (1998) Two generations of diamonds in the eclogite xenoliths. 7th Int Kimberlite Conf Abstr, p 844–846
Stachel T, Harris JW (2008) The origin of cratonic diamonds; constraints from mineral inclusions. Ore Geol Rev 34:5–32
Stachel T, Luth RW (2015) Diamond formation; where, when and how? Lithos 220–223:200–220
Stachel T, Brey GP, Harris JW (2005) Inclusions in sublithospheric diamonds; glimpses of deep earth. Elements 1:73–87
Stachel T, Banas A, Muehlenbachs K, Kurszlaukis S, Walker EC (2006) Archean diamonds from Wawa (Canada); samples from deep cratonic roots predating cratonization of the Superior Province. Contrib Mineral Petrol 151:737–750
Stachel T, Aulbach S, Harris JW (2022) Mineral inclusions in lithospheric diamonds. Rev Mineral Geochem 88:307–392
Sumida N, Lang AR (1981) Cathodoluminescence evidence of dislocation interactions in diamond. Philos Mag A 43:1277–1287
Sunagawa I (1995) The distinction of natural from synthetic diamonds. J Gemmol 24:485–499
Sutton JR (1928) Diamond: A Descriptive Treatise. T. Murby
Suzuki S, Lang AR (1976) Internal structures of natural diamonds revealing mixed-habit growth *In:* Diamond Research. Daniel P (ed) Industrial Diamond Information Bureau, Ascot, England, p 39–47
Tacy (2018) 2018 Tacy's Diamond Pipeline:
https://www.thediamondloupe.com/sites/awdcnewswall/files/attachments/TacyPipeline_TheDiamondLoupe_bis.pdf
Tappert R, Tappert MC (2011) Diamonds in Nature: A Guide to Rough Diamonds. Springer-Verlag, Berlin
Taylor WR, Canil D, Milledge HJ (1996) Kinetics of Ib to IaA nitrogen aggregation in diamond. Geochim Cosmochim Acta 60:4725–4733
Timmerman S, Chinn IL, Fisher D, Davies GR (2018) Formation of unusual yellow Orapa diamonds. Miner Petrol 112:209–218
Titkov SV, Krivovichev SV, Organova NI, Mills S (2012) Plastic deformation of natural diamonds by twinning; evidence from X-ray diffraction studies. Mineral Mag 76:143–149
Vance ER, Milledge HJ (1972) Natural and laboratory alpha-particle irradiation of diamond. Mineral Mag 38:878–881
Vance ER, Harris JW, Milledge HJ (1973) Possible origins of alpha-damage in diamonds from kimberlite and alluvial sources. Mineral Mag 39:349–360
Walter MJ, Thomson AR, Smith EM (2022) Geochemistry of silicate and oxide inclusions in sublithospheric diamonds. Rev Mineral Geochem 88:393–450
Welbourn CM, Rooney MLT, Evans DJF (1989) A study of diamonds of cube and cube-related shape from the Jwaneng Mine. J Cryst Growth 94:229–252
Welbourn CM, Cooper M, Spear PM (1996) De Beers natural versus synthetic diamond verification instruments. Gem Gemol 32:156–169
Westerlund KJ, Gurney JJ, Carlson RW, Shirey SB, Hauri EH, Richardson SH (2004) A metasomatic origin for late Archean eclogitic diamonds; implications from internal morphology of diamonds and Re–Os and S isotope characteristics of their sulfide inclusions from the Late Jurassic Klipspringer kimberlites. S Afr J Geol 107:119–130
Wiggers de Vries DF, Bulanova GP, de Corte K, Pearson DG, Craven JA, Davies GR (2013) Micron-scale coupled carbon isotope and nitrogen abundance variations in diamonds; evidence for episodic diamond formation beneath the Siberian Craton. Geochim Cosmochim Acta 100:176–199
Williams AF (1932) The Genesis of Diamond. Two Volumes. Ernest Benn Ltd., London
Wulff G (1901) On the question of speed of growth and dissolution of crystal surfaces. Z Kristallogr 34:449–530 (in German)
Yacoot A, Moore M (1993) X-ray topography of natural tetrahedral diamonds. Mineral Mag 57:223–230
Yacoot A, Moore M, Machado WG (1998) Twinning in natural diamond. I. Contact Twins. J Appl Crystallogr 31:767–776
Yamaoka S, Komatsu H, Kanda H, Setaka N (1977) Growth of diamond with rhombic dodecahedral faces. J Cryst Growth 37:349–352
Yamaoka S, Kanda H, Setaka N (1980) Etching of diamond octahedrons at high temperatures and pressure with controlled oxygen partial pressure. J Mater Sci 15:332–336
Yelisseyev AP, Pokhilenko NP, Steeds JW, Zedgenizov DA, Afanasiev VP (2004) Features of coated diamonds from the Snap Lake/King Lake kimberlite dyke, Slave Craton, Canada, as revealed by optical topography. Lithos 77:83–97
Zedgenizov DA, Harte B, Shatsky VS, Politov AA, Rylov GM, Sobolev NV (2006) Directional chemical variations in diamonds showing octahedral following cuboid growth. Contrib Mineral Petrol 151:45–57
Zedgenizov DA, Kalinina VV, Reutsky VN, Yuryeva OP, Rakhmanova MI, Shirey SB (2016) Regular cuboid diamonds from placers on the northeastern Siberian Platform. Lithos 265:125–137
Zhan Z (2020) Mechanisms and implications of deep earthquakes. Annu Rev Earth Planet Sci 48:147–174
Zhang Z (2016) Diamond resorption morphology as a fluid proxy in diamond-bearing environments: constraints from empirical and experimental studies. PhD Dissertation, Dalhousie University, Halifax, Canada
Zhang Z, Fedortchouk Y, Hanley JJ (2015) Evolution of diamond resorption in a silicic aqueous fluid at 1–3 GPa; application to kimberlite emplacement and mantle metasomatism. Lithos 227:179–193